



Title	An early warning criterion for the prediction of snowmelt-induced soil slope failures in seasonally cold regions
Author(s)	Subramanian, Srikrishnan Siva; Ishikawa, Tatsuya; Tokoro, Tetsuya
Citation	Soils and foundations, 58(3), 582-601 https://doi.org/10.1016/j.sandf.2018.02.021
Issue Date	2018-06
Doc URL	http://hdl.handle.net/2115/78324
Rights	© 2018. This manuscript version is made available under the CC-BY-NC-ND 4.0 license http://creativecommons.org/licenses/by-nc-nd/4.0/
Rights(URL)	http://creativecommons.org/licenses/by-nc-nd/4.0/
Type	article (author version)
File Information	paper_S&F 2018 58(3) author_version-1.pdf



[Instructions for use](#)

**An early warning criterion for the prediction of snowmelt induced soil slope failures in
seasonal cold regions**

Srikrishnan Siva Subramanian ⁱ⁾, Tatsuya Ishikawa ⁱⁱ⁾ and Tetsuya Tokoro ⁱⁱⁱ⁾

ⁱ⁾ Srikrishnan Siva Subramanian,

Post-Doctoral Researcher

Laboratory of Analytical Geomechanics, Faculty of Engineering, Hokkaido University, Kita 13, Nishi 8,
Kita-ku, Sapporo, Hokkaido, 060-8628, Japan

e-mail: srikrishnan@frontier.hokudai.ac.jp and srikrishnansharma@gmail.com

ⁱⁱ⁾ Tatsuya Ishikawa (**Corresponding author**)

e-mail: t-ishika@eng.hokudai.ac.jp

Professor, Faculty of Public Policy, Hokkaido University, Japan

ⁱⁱⁱ⁾ Tetsuya Tokoro

Associate Professor, Department of Civil Engineering, National Institute of Technology, Tomakomai
College, Tomakomai, Hokkaido, Japan

e-mail: t-tokoro@tomakomai-ct.ac.jp.

ABSTRACT

In Hokkaido Japan, soil slope failures occur frequently during snow melting season. These slope failures are triggered by the excess amount of water derived from the snowmelt and rainfall. For the prediction of snowmelt induced soil slope failures in seasonal cold regions, an early warning criterion is required. The existing Japanese early warning criteria for sediment disasters i.e. 60-minute cumulative rainfall and Soil-Water-Index (SWI) relationships, effective rainfall indexes etc. consider the influence of rainfall and time-dependent random moisture of the soil. These criteria do not consider the soil moisture contributed by the snowmelt water. In this study, the applicability of the existing early warning criteria to predict the snowmelt induced soil slope failures are examined. An empirical method to quantify the amount of snowmelt water is presented. Various scenarios of conceptual soil slope failures are studied using numerical simulations under different magnitudes of rainfall and snowmelt water. As a result, a revision for the SWI and effective rainfall index incorporating the amount of snowmelt water with rainfall is introduced and the slope failure scenarios are studied. Based on the results, a new early warning criterion Effective Precipitation index is introduced. It is found that the new failure criteria introduced in this study perform well for the prediction of snowmelt induced soil slope failures.

Keywords: Snowmelt water, seasonal cold regions, soil slope stability, soil-water index, effective rainfall index, early warning systems (IGC: E06/E09/E13)

INTRODUCTION

In seasonal cold regions, the climate effects i.e. freeze-thaw action and snowmelt water infiltration affect the moisture content of the soil (Ishikawa et al. 2015). The snowmelt water infiltrated into the soil ground through a long period results in large amount of surface water and may trigger landslides and debris flows (Nakatsugawa et al. 2015). The stability of soil slopes in seasonal cold regions are more sensitive to the amount of snowmelt water and ignoring the effect of snowmelt may not properly judge the stability (Siva Subramanian et al. 2017). Many studies have been done to standardise an early warning criterion to predict the oncoming slope disasters in snowy cold regions by using metrological data i.e. rainfall and snowmelt water etc. (Okimura and Ichikawa, 1985, Berris and Harr 1987, Singh et al. 1997, Williams et al. 1999, Matsuura 1998, Matsuura 2000, Matsuura et al. 2005, Matsuura et al. 2008, Matsuura et al. 2013 and Nakatsugawa et al. 2015). According to many of the above-mentioned studies, the Japanese early warning criteria i.e. Soil-water index (SWI) and Effective rainfall index (ER) etc. need to be revised for the prediction of slope failures in seasonally cold regions. These criteria do not consider the soil water content supplied from the snowmelt. Compared to the hourly rate of rainfall precipitations, the hourly rate of snowmelt water is relatively very small. Instead, the snowmelt process is continuous during thawing season resulting in a continuous supply of water to the soil surface. The indistinct infiltration behaviour of snowmelt water is studied by many researchers (Komarov and Makarova 1973, Matsuura, 1998, Ishida et al. 2000 and Iwata et. al. 2011). Snowmelt infiltration processes are affected by many factors i.e. soil temperature, soil freezing depth, water content of soil before winter and depth of snow cover (Iwata et. al. 2011). Due to the presence of thick snow cover, most of the soil ground beneath the snow will experience a shallow freezing depth. Komarov and Makarova (1973) showed that a shallow freezing depth induces a large snowmelt water infiltration. Matsuura (1998) compared the hourly rate of snowmelt water with rainfall over a mountainous region Busuno, Japan and found the maximum hourly snowmelt rate would be 15 mm/hr. This maximum value of water is very less compared to rainfall. Due to these facts, there is a

possibility of continuous infiltration of snowmelt water into the soil. As the snowmelt water infiltration is continuous and its effects on soil slope instabilities are distinct, the above-mentioned criteria SWI and ER fail to predict the oncoming soil slope failures and debris flows due to the larger pre-determined threshold for heavy rainfall. For these reasons, a method to quantify the hourly rate of snowmelt is necessary so that it can be incorporated in these early warning criteria. Based on this background, a criterion which can be used for the early warning of soil slope failures and debris flow disasters is proposed in this study. Two case studies of soil slope failures occurred in Hokkaido are studied. The applicability of the existing early warning systems is studied by applying those criteria to the case studies. An empirical method to estimate the hourly snowmelt rate is presented. A new early warning criterion to predict the snowmelt induced soil slope failures in seasonal cold regions is introduced. The applicability and validity of the new criterion is examined through detailed parametric numerical simulation studies.

SOIL SLOPE INSTABILITIES IN SEASONAL COLD REGIONS

In this study, many case examples of soil slope failures occurred in Hokkaido, Japan have been studied. Table 1 summarizes a list of sediment disasters occurred during thawing seasons in Hokkaido from 1999 to 2013. For example, on 07-04-2013 (dd-mm-yyyy), at 11:20 A.M., a slope failure happened along the national highway route 230 in Hokkaido, Japan as shown in Figure 1 (a). The national highway connects Sapporo city of Hokkaido with Setana, a town in the Hiyama subprefecture of Hokkaido. Hereafter, the slope failure will be referred as highway slope failure in this paper. The slope failure occurred at the embankment along the roadway. The size of the slope failure was 44 m in length and 19 m in height. Approximately 11000 m³ of sediment containing embankment filling material and accumulated snow above the soil ground together flowed out downward to the slope foot as shown in Figure 1 (a). The slope failure has been induced by the combined action of heavy rainfall and snowmelt water (Hokkaido Regional Development Bureau, 2014). The cumulative daily rainfall occurred on the day of slope failure is 92 mm and the cumulative snowmelt is 31 mm as recorded in a nearby meteorological telemetry

maintained by Ministry of Land, Infrastructure, Transport and Tourism, Hokkaido Regional Development Bureau (MLIT). This data is collected from a nearby meteorological telemetry which is closest to the disaster site as depicted in Figure 1 (a). The snowmelt water is not measured physically using a snow lysimeter etc. The amount of snowmelt water (SM) directly corresponds to the snow water equivalent (SWE), the reduced snow depth (SD) and the density of snow (ρ_{sn}). On an average, previous studies have shown that the maximum density of snow (ρ_{sn}) in Hokkaido would be 500 kg/m^3 (Abe and Shimizu, 2009). Based on this, the amount of snowmelt water is estimated from the snow depth data recorded at the telemetry as half the amount of the reduced accumulated depth of the snow during 07-04-2013 according to the following relationship.

$$SM = \frac{\rho_{sn}}{\rho_w} \times \Delta SD \quad (1)$$

SM = snowmelt water (mm), ρ_{sn} = density of snow (kg/m^3), ρ_w = density of water (kg/m^3) and ΔSD = the amount of decrease in accumulated snow depth (mm). In this case, the density of snow is assumed constant as 500 kg/m^3 with reference to the study of Abe and Shimizu (2009) and the density of water is assumed to be 1000 kg/m^3 . Using Equation (1) both the cumulative as well as hourly snowmelt water can be estimated. The maximum hourly rainfall recorded on 07-04-2013 is 12 mm as given in Figure 1 (b). The rainfall has been continuous from 07-04-2013 00:00 to 07-04-2013 11:00. The rainfall occurred on 07-04-2013 is the maximum that was recorded in the century. The cumulative daily rainfall along with the cumulative snowmelt water together amounted a total of 123 mm and caused the slope failure.

In addition to the snowmelt induced soil slope failures mentioned above, many occurrences of rainfall induced slope failures were also reported in Hokkaido. It is indispensable to discuss the applicability of early warning criteria for the prediction of rainfall induced soil slope failures as well as snowmelt induced soil slope failures. Therefore, a series of rainfall induced sediments disasters happened along many of the expressways and national highways of Hokkaido during August 2016, by Typhoon 10

were studied. Figure 2 show some of the large-scale sediment disasters captured along Doto expressway and National Highway route 274. The maximum amount of cumulative rainfall occurred in some stations exceeded 700 mm within just 3 days of typhoon. The rainfall recorded during the typhoon at three different meteorological telemetries Nissho pass, Karikachi pass and Nozuka pass are shown in Figure 3. The rainfall has been continuous from 28-08-2016 17:00 to 31-08-2016 03:00. The maximum hourly rainfall occurred on 31-08-2016 00:00 at Nissho and Karikachi stations are 55 mm, 38 mm respectively. At Nozuka pass the maximum recorded hourly rainfall was 34 mm on 30-08-2016 19:00. The maximum cumulative rainfall during the typhoon was about 713 mm recorded at Nozuka pass telemetry as shown in Figure 3(c). At other telemetries Nissho and Karikachi pass 488 mm and 364 mm of cumulative rainfall were recorded. Among all those case examples discussed, a recent slope failure named as Nakayama pass slope failure and the case example of series of sediment disasters induced by the Typhoon 10 are chosen for elaborate studies.

SOIL WATER INDEX (SWI) AND EFFECTIVE RAINFALL INDEX (ER) RELATIONSHIPS

For the prediction of slope failures in cold regions, whose mechanism is different from warm region slope failures and rainfall induced slope failures, a stability criterion or an early warning system should consider at least some of the influencing factors like freeze-thaw action, snowmelt water infiltration etc. so that a proper warning can be made. For the prediction of rainfall induced slope failures, the Soil Water Index (SWI) is widely used by Japanese Meteorological Agency (JMA) and the effective rainfall index (ER) is used by East Japan Railway Company (JR East). Whereas, the slope failures in seasonally cold regions like Hokkaido are not only influenced by the rainfall. There are other factors than the rainfall to induce a slope failure in cold regions. In consideration to these aspects, a method to predict the soil slope failures in cold regions is developed in this study.

Relationship between 60-minute cumulative rainfall and Soil Water Index (SWI)

In Japan, Japanese Meteorological Agency (2012) performs the early warning of slope failures induced by the rainfall based on the relationship between 60-minute cumulative rainfall and Soil Water Index (SWI) (Osanai et al. 2010). The calculation of 60-minute cumulative rainfall and Soil-water index is referred from Okada, (2001). The Soil Water Index is a concept model that uses a calculated value of the total water depth of a three-layer tank model estimated using the coefficients of the model as given in Figure 4.

According to the research of Okada (2001), the Soil–Water Index remains unchanged in many cases even when the parameters of the tank model are changed. The fixed parameters are identified by statistical analysis as confirmed by Okada (2001) for the relationship between rainfall and discharge in a Granite region in Japan as listed in Figure 4. The inflow for the model includes the rainfall amount of the target period. The outflow from the model is calculated based on the equations below.

$$q_1(t) = \alpha_1 \{S_1(t) - L_1\} + \alpha_2 \{S_1(t) - L_2\} \quad (2)$$

$$q_2(t) = \alpha_3 \{S_2(t) - L_3\} \quad (3)$$

$$q_3(t) = \alpha_4 \{S_3(t) - L_4\} \quad (4)$$

Standing water in each tank is represented as,

$$S_1(t + \Delta t) = (1 - \beta_1 \Delta t) \times S_1(t) - q_1(t) \times \Delta t + R \quad (5)$$

$$S_2(t + \Delta t) = (1 - \beta_2 \Delta t) \times S_2(t) - q_2(t) \times \Delta t + \beta_1 \times S_1(t) \times \Delta t \quad (6)$$

$$S_3(t + \Delta t) = (1 - \beta_3 \Delta t) \times S_3(t) - q_3(t) \times \Delta t + \beta_2 \times S_2(t) \times \Delta t \quad (7)$$

$$SWI = S_1 + S_2 + S_3 \quad (8)$$

where α_1 , α_2 , α_3 and α_4 are the outflow coefficients of the tanks; L_1 , L_2 , L_3 and L_4 are the heights of the outflow holes of the tanks; β_1 , β_2 and β_3 are the penetration volumes of the tanks; R is the cumulative hourly rainfall, t is current time and Δt is time step and in this case, it is 60 minutes. For the early warning of debris flows and slope failures, JMA uses a threshold line as a criterion for the relationship between

60-minute cumulative rainfall and Soil-water index. The concept of the early warning system currently adopted in Japan (Osanai et al. 2010) is given in Figure 5. The applicability of these criteria for the slope failures induced in seasonal cold regions due to the various influencing factors as discussed in this study should be verified.

60-minute cumulative rainfall and Soil Water Index relationships (SWI) for the soil slope failure occurred on April 2013 along National Highway Route 230 is calculated and shown in Figure 6. Calculated 60-minute cumulative rainfall and SWI are based on the method given by Okada (2005). The CL for each region in Japan is determined based on the occurrences and non-occurrences of sediment disasters corresponding to a value of 60-minute rainfall and Soil Water Index (Osanai et al. 2010). Critical Line (CL) designated for Hokkaido is referred from Nakatsugawa et al. (2015). As the CL is determined only based on the occurrence of disasters induced by rainfall, it could not consider the long-term snowmelt water infiltration and cannot be used to predict the snowmelt induced slope failures. Iwakura et al. (2010) calculated the 60-minute cumulative rainfall and SWI assuming a 2 mm/hr. constant value for snowmelt water for three different slope failures occurred in Hokkaido. In this study, instead of considering an assumed constant amount of snowmelt water, the snowmelt water will be estimated empirically as discussed in the following section 4. Further as there was no slope failure predicted by the existing CL Iwakura et al. (2010) attempted to define a new CL by reducing the threshold values of 60-minute rainfall and Soil Water Index. Similarly, in this study the CL threshold is never reached for the slope failure cases. The reasons could be due to the negligence of snowmelt water and the threshold level is much higher. Due to the slow infiltration rate of snowmelt water, the high CL thresholds are never reached. On the other hand, the rainfall data of the slope failures occurred in the snowmelt seasons are included to define the CL in SWI. However, the ultimate value of hourly rainfall alone is not enough to reach the CL (for many case examples of slope failures in Hokkaido). This is because, for slope failure disasters induced by rainfall (i.e. heavy rain and typhoon) a maximum amount of hourly rainfall on an

average about 50 to 60 mm/hr is recorded. Whereas, by observing the climate data of Hokkaido for the last decade emphasis that such high hourly rainfall never happened during snowmelt season. Due to these facts it is very clear that incorporation of snowmelt water and a new CL for SWI would be necessary. On the other hand, 60-minute cumulative rainfall and Soil Water Index relationships (SWI) for the climate data collected from Nissho pass, Karikachi pass and Nozuka telemetries are calculated as shown in Figure 7. The timeframe is set as 01-04-2016 up to August 31, 2016 to visualise at what occasions the CL is exceeded and to validate it against the actual slope failure data. For the sediment disasters induced by the Typhoon during August 2016, the occurrences are predicted and the snake lines exceeds the CL for location Nissho pass and Nozuka pass telemetries. Whereas for the Karikachi pass, the CL is not exceeded. Similar cases in which the threshold for SWI is higher were met during the 2016 typhoon on prefectures like Nara and Wakayama. JMA proposed lowering the threshold values up to 50 % to 80 % for these places (JMA, 2016). On an average, the threshold level could be considered applicable to predict such large amount of rainfall disasters in Hokkaido. From this observation, it is very clear that the 60-minute cumulative rainfall and Soil-Water-Index relationships are applicable for the prediction of large sediments disasters induced by heavy rainfall and may not predict the slope failures induced by snowmelt water. The existing threshold level designated for Hokkaido is not applicable and not realistic for the prediction of snowmelt induced soil slope failures.

Effective rainfall index

The effective rainfall index is calculated based on the below given method. In the conventional method given by Yano (1990), two half-lives i.e. 1.5 hours and 24 hours were used. The effective rain is then calculated as follows,

$$ER = [(\sum \alpha_{1i}) \times R_{1i}] \quad (9)$$

ER = Effective rainfall (mm), $\alpha_{ii} = 0.5^{i/T}$ the reduction coefficient i hours beforehand, R_{1i} = current 1-hour rainfall amount (mm/hr.) and T = half-life.

There are various half-life periods determined i.e. 1.5 hours, 6 hours, 24 hours and 72 hours. Sudden heavy rainfall exceeding 30 mm/hr. rate will result in shallow and surface erosion type slope failures which can be predicted using effective rainfall with half-lives 1.5 hours and 6 hours or 24 hours. Large slope failures like deep seated landslides, which result from continuous surface infiltration due to small to medium amount of rainfall (0 - 30 mm/hr.) can be predicted using 72 hr. half-life. Matsuura et al. (2013) have suggested the use of 72 hours half-life along with 1.5 hours half-life, so that the slow infiltration process of snowmelt water can be accounted. The critical line (CL) for this effective rainfall index is determined based on the occurrence of small to large scale sediment disasters observed in a mountain area at Busuno, Japan during the snowmelt seasons (Matsuura et al. 2013). The effective rainfall of a 72 hours half-life time on the X-axis and effective rainfall of 1.5 hours on the Y-axis are used as the standard rainfall indexes in this study with reference to Matsuura et al. (2013).

The ER index is applied to the Nakayama pass slope failure as shown in Figure 8. The slope failure is not predicted as the snake lines are just below the CL. The reason could be the non-consideration of snowmelt water. Even if the half-life of the ER is changed to either 6 hours or 24 hours instead the 72 hours, the slope failure is still not predicted. The ER based on 1.5 hours and 72 hours half-lives are calculated for the climate data obtained from Nissho, Karikachi and Nozuka pass telemetries and as shown in Figure 9 (a), (b) and (c). It could be seen from Figure 9 that for all the cases of climate data sets recorded for the typhoon rainfall, the criteria are applicable and many occurrences of sediments disasters are predicted. For the case of Nissho pass telemetry and Nozuka pass telemetry data, the CL is exceeded on August 23, 2016 and July 28, 2016 respectively, though there are no slope failures recorded at that time. Since the CL threshold set by Matsuura et al. (2013) is small compared with the CL set for rainfall induced slope failures i.e. Yano (1990), Senoo et al. (2001) and Tereda and Nakaya (2001), the

line can be exceeded with considerable amount of rainfall. At any case the CL set by Matsuura et al. (2013) is also on the safer side. In this aspect, it may be necessary to establish a different CL for rainfall induced slope failures in cold regions. Tereda and Nakaya (2001) have established some guidelines to set CL for rainfall induced slope failures using 1.5 hr. and 72 hr. half-lives. In their research, they superimpose the Y axis with 1.5 hr. half-life of ER instead 1 hr. half-life and keep the X axis 72 hr. half-life and validated the CL threshold against actual slope failure cases. Following the guideline by Tereda and Nakaya (2001), in this study four different CLs proposed by Yano (1990), i.e. CL1, CL2, CL3 and CL4 shown in Figure 9 have been used. Of those 4 CLs, Yano (1990) recommends the use of CL3 for the Nikko area in Tochigi prefecture. To check the appropriateness of the CLs proposed by Yano (1990), in this study all the 4 CLs are used for the cases of rainfall induced slope failures. It could be seen that the CLs lines set by Yano (1990) delineates the slope failure for the Typhoon 10 more clearly. According to the research by Senoo et al. (2001), the standard CL for effective rainfall index for rainfall induced disasters varies significantly based on the area. Senoo et al. (2001) have analysed the difference in CL among areas i.e. Fukushima, Sado and Kochi. In this aspect, the CLs proposed by Yano (1990) for Nikko area in Tochigi prefecture should be validated for its use in Hokkaido prefecture.

From these observations, it is very clear that different CLs are required for both SWI and ER to predict the snowmelt induced slope failures. In general, rather than the threshold level for the SWI, the threshold level designated for the ER seems to be applicable for both rainfall and snowmelt induced soil slope failures since there are different CLs available for both the cases. For the case study of Nakayama pass slope failure, the disaster is not predicted from both the criteria SWI and ER. The major reason could be due to the negligence of snowmelt water. It is very clear that a proper estimation of snowmelt water is required for the precise prediction of snowmelt induced soil slope failures in seasonal cold regions.

SNOWMELT SIMULATION

The estimation of hourly rate of snowmelt is necessary for early warnings. Use of many energy balance methods are common in practice (Berris and Harr, 1987; Kondo and Yamazaki, 1990). In this study, a simple yet reliable estimation method of the snowmelt water is introduced which considers almost all the physical processes included in the melting process of snow (Riley et al. 1969). The method could be termed as an analytical method. The key influencing climatic factors are considered i.e. air temperature, snow surface temperature, melt factor etc. Climate data obtained from the Automatic Meteorological Data Acquisition System (AMeDAS) (JMA) is used for the estimations. For the estimation of snowmelt water from the meteorological data, a method is employed considering the physical process of snowmelt (Riley et al. 1969, Motoyama, 1990) as given below,

$$SM = 0.4 \times SD \times RI \times (T_a - T_{st}) \times (1 - Al) + \left[(T_a - T_{st}) \times \frac{P}{144} \right] \quad (10)$$

where SM = hourly snowmelt water per increment in air temperature (mm/hr.°C), T_a = air temperature (°C), T_{st} = snow freezing temperature (°C), SD = hourly amount of decrease in depth of snow cover (mm/hr.), RI = Radiation Index (%), Al = Albedo (%) and P = Precipitation (mm/hr.). The hourly snowmelt is determined based on the increment in air temperature for every one-hour duration (Riley et al. 1969).

The model adopted for the estimation of snowmelt water is calculated using Equation 10 and the concept is shown in Figure 10. As shown in the figure the model considers the snow density, melt factor and liquid water holding capacity of snowpack etc. explicitly. Any early warning method for landslides/sediment disasters is based on meteorological data that is to the most precise to the disaster site obtained from installed meteorological telemetries/stations. In this study, the early warning is based on the physical conditions of the region and cannot be of respective slope because it is practically not possible to obtain individual snow depth data for each slope unless snow depth gauge is manually installed at the targeted region. Due to this fact, the snow depth measurement can only be directly

obtained from the field or any meteorological observatory/telemetry. The snowmelt model is used to estimate the amount of snowmelt water for the case of Nakayama pass slope failure. The results are shown in Figure 11 (b) and (c). A total of 31 mm snowmelt water is estimated on 07-04-2013 using the model. Hokkaido regional development bureau (mentioned as MLIT in Figure 11) estimated the cumulative snowmelt water on 07-04-2013 to be 31 mm. The total cumulative snowmelt water estimated using the model matches with the estimation of MLIT. On the other hand, to validate the snowmelt model, a comparison of the estimated snow depth to the measured snow depth data for the Nakayama pass slope failure starting from 01-11-2012 to 07-04-2013 is made as shown in Figure 11 (b). The estimated results from the snowmelt model also match well with the measured results. From these observations, the snowmelt model may be reliable to estimate the hourly snowmelt water.

PARAMETRIC STUDIES OF SOIL SLOPE FAILURES UNDER DIFFERENT MAGNITUDES OF RAINFALL AND SNOWMELT WATER

For the revisions/proposal of early warning criteria, many numbers of soil slope failures should be examined to check the appropriateness and applicability. On the other hand, it is time consuming and cumbersome to collect data and study in detail many slope failure case examples. In consideration to these aspects, many conceptual soil slope failures are studied using numerical simulations based on a recommended slope stability assessment approach. The applicability and validity of the numerical simulation method is detailly examined by Siva Subramanian et al. (2017). In this study, an embankment slope model made up of a volcanic soil is chosen for the parametric studies due to the fact that volcanic soils are spread all over Japan and especially in Hokkaido 40 % of the surface is occupied by various types of volcanic soils. The soil material properties considered are same as the previous study. In the previous study, the simulation was performed for a duration of 373 days starting from 09-11-2012 to 17-10-2013. Further details about the embankment slope and its numerical simulations can be found from Matsumura (2014), Kawamura et al. (2016) and Siva Subramanian et al. (2015). In this study, the

numerical analyses were done with different initial water content distributions chosen from different time. Those cases are as listed in Table 2. The slope geometry and boundary conditions are shown in Figure 12. Initial volumetric water content distributions and temperature distributions for the parametric studies are shown in Figure 13 and Figure 14 respectively. The primary variables considered in the parametric study are the initial water content distribution chosen from day 100, 150, 200 and 343. The slope height (H), the slope angle (α), different rainfall (P_r) and snowmelt rates (P_s) considered are summarised in Table 3 and Table 4. Different combinations of rainfall and snowmelt water are applied as given below.

- Long-term rainfall with low 60-minute rainfall amount with and without snowmelt water
- Short-term rainfall with high 60-minute rainfall amount with and without snowmelt water
- Long-term and short-term rainfall with slow snowmelt rate and rapid snowmelt rate

The following conditions are adopted as shown in Table 4.

- For long term rainfall, the duration is considered as 24 hours. The amount of rainfall is considered as 10 mm/hr.
- For short term rainfall, the duration is considered as 6 hours. The rainfall amount is considered as 30 mm/hr.
- Two different snowmelt rates are considered 4 mm/hr. (slow snowmelt rate) and 15 mm/hr. (rapid snowmelt rate) in consideration to some extensive field studies (Matsuura, 1998).
- The duration of the snowmelt is considered as 24 hours in which the snowmelt is assumed to be a sinusoidal function. At 12:00 noon the snowmelt rate is at the maximum.

As found from the previous studies (Ishikawa et al. 2015 and Nakatsugawa et al. 2015) the macro factor that influence the soil slope stability in snowy cold regions are the amount of rainfall and snowmelt water. Various magnitudes of rainfall and snowmelt water are considered under different influential conditions and the stability scenarios are studied. Different slope angles were considered, 30°, 35°, 40° and 45° with different slope heights 5 m, 10 m, 15 m and 20 m as shown in Table 3. Table 3 also shows the summary of

analytical conditions of selected slope models with different slope angles. The different infiltration boundary conditions are shown in Table 4. The series are named as A, B, C and D based on the initial conditions. The rainfall boundary conditions are named as a, b, c, d and e with the snowmelt rates as (i), (ii) and (iii) respectively. A total number of 960 numerical simulations were performed, of those 512 numbers of slope failures and 448 numbers of stable scenarios were obtained. These stable and failure scenarios are used for the revision and proposal of early warning criteria as discussed in section 6. The results of all the 960 numerical slope failure cases for each series are summarised in Appendix in Tables A1, A2, A3 and A4 for series A, B, C and D respectively.

REVISIONS/PROPOSAL OF NEW EARLY WARNING CRITERIA

Possible revisions of the early warning criteria are studied by incorporating the amount of snowmelt water along with rainfall in both the SWI and ER indices. Revisions of the effective rainfall index, 60-minute rainfall and SWI relationships are studied through;

1. Including snowmelt water in ER/SWI calculation
2. Determining/revising the threshold – Critical Line (CL)

The revisions of the early warning are done for the slope failure scenarios observed from the conceptual numerical slope failure cases. From those simulations performed as explained in section 5, the failure as well as stable scenarios are classified based on the factor of safety value (FOS). The FOS values lower than 1 are considered as slope failures.

Proposal of new criteria Effective Precipitation (EP) index

For all the failure and stable scenarios obtained from the simulations, the Effective Precipitation index and Soil Water Index were calculated. The method to calculate the EP index is explained as follows. The slope disasters occur in seasonal cold regions are influenced by the short-term and long-term soil surface infiltration caused by the rainfall and continuous snowmelt process respectively. In this study, a new

criterion to predict the snowmelt induced soil slope failures, considering the short-term and long-term soil surface infiltration is proposed. The new criterion Effective Precipitation index (EP) considers the rainfall and snowmelt water by adopting two half-lives namely 1.5-hour half-life and 72-hours half-life and can be calculated as,

$$EP = P_t + \sum [P_{t-n} \times 0.5^{n/T_h}] \quad (11)$$

where, EP = Effective Precipitation (mm), P_t = the 1-hour precipitation (rainfall and snowmelt water) at the present time (mm/hr.), P_{t-n} = the precipitation recorded n hours beforehand (mm/hr.) and T_h = the half-life time (hours). The precipitation P_t includes the hourly rainfall as well as the hourly snowmelt water. The proposed criteria EP index is similar to the MR proposed by Matsuura et. al. (2013). Matsuura et al. (2013) considered the snowmelt water in their calculation by setting up monitoring stations in Busuno, Japan. On the other hand, it is never possible to set up monitoring stations all over the targeted area (i.e. Hokkaido). To overcome such intricacy, in this study the hourly snowmelt water is estimated from the snowmelt estimation method given in section 4. If an early warning criteria should be adopted for Hokkaido region, many case examples of slope failures should be studied considering different snowmelt and rainfall rates. Further, Matsuura et al. (2013) have shown only one case of slope failure during snowmelt season and two cases of slope failures during rainy seasons from which it will be difficult to adapt the concept of MR all over Hokkaido. Considering all these aspects in this study a criteria EP index is proposed and validated against many cases of slope failures.

Effective precipitation index 1.5 hours and 72 hours considering snowmelt water is shown in Figure 15 for the Nakayama pass slope failure. It could be seen that the criteria successfully predict the slope failure as the snake line exceeding the Critical Line (CL) proposed by Matsuura et al. (2013). Additionally, the effective precipitations are studied for the numerical parametric studies as shown in Figure 17 and Figure 18. These two figures are arranged like, in the left the factor of safety (FOS) obtained from the simulations, in the centre EP index and in the right SWI for the corresponding cases.

The stability of the slope is inferred from FOS values in the left figures. Then, the middle and right figures are checked whether the criteria predict the slope failure or not. In Figure 17, there are two cases in which slope failure occur. The slope failures occur at times 19:00 for case a(ii) and at 12:00 for case a(iii). For both the cases the EP predicts the slope failure as the CL is exceeded. In this way, the applicability of the EP and SWI are checked and validated. In other words, it could be described that, once the CL is exceeded there is a danger of slope failure and since the EP value continue to increase with time a failure is observed. The soil slope failures usually will get triggered after some considerable duration of rainfall. Owing to these conditions, the prediction by the EP index would also be considered appropriate. It could be seen that for most of the cases of failures and stable scenarios the criteria perform well for the cases in Figure 17 and Figure 18. The Effective Precipitation index for half-lives 6 hours and 24 hours were also plotted in Figure 19 and Figure 20 to compare it with 72 hours effective precipitation. For the case of slope failures in Figure 19, the Effective Precipitation with half-lives 6 hours and 24 hours do not predict the slope failure. Table 5 shows the number of slope failures and stable cases for each series and the rate of predictions by EP using three different half-lives. The number of slope failures observed in each series A, B, C and D are 0, 224, 224 and 64 respectively (total 512). It could be seen that for all the slope failures during thawing and after thawing seasons (series B and C), the EP with 72 hours half-life gives 100 % prediction whereas the EP with half-lives 6 hours and 24 hours give 86.66 % of successful predictions. Only for the case of failures induced by high amount of rainfall and snowmelt water, the slope failure is predicted by 6 hours and 24 hours half-lives as shown in Figure 21. In all these situations, the applicability of 72 hours half-life Effective Precipitation was found to be appropriate. From this observation, it could be said that for the prediction and early warning of snowmelt induced soil slope failures, the proposed new criteria with half-lives of 1.5 hours and 72 hours will be helpful. On the other hand, it is noteworthy to discuss the trend of false predictions (stable cases predicted as failures) by the EP index so that the limitations of the criteria can be understood. As shown in Table 6, the rate of false

predictions is calculated for series A, B, C and D using CL defined by Matsuura et al. (2013) and CL3 defined by Yano (1990). All the slopes were stable in series A (during freezing) and 176 numbers of stable cases were observed in series D (before freezing). Since the threshold value (CL proposed by Matsuura et al. 2013) of the EP index is low for all these stable cases, the CL will be exceeded and a false warning may be made. Whereas if the CL3 proposed by Yano (1990) is used, the false warnings can be avoided as shown in Table 6. Similar trend was also observed for the cases of Typhoon disaster in Hokkaido using the ER index discussed in section 3.2. Different critical lines (CL) are necessary during rainfall season and snow melting and thawing season. For the cases of series B and C (thawing and after thawing seasons), there are no false warnings observed. All the slope failures are predicted as failures and all the stable cases were also identified properly. It could be said that the CL proposed by Matsuura et al. (2013) designated using the EP index is especially applicable for soil slope failure in snow melting and thawing season and after thawing season. Whereas for the case of rainfall induced slope failures the CL proposed by Yano, (1990) is found applicable. Figure 21(a) and (b) show the Effective Precipitation index for all the numerical case examples for series B and C and series A and D respectively. These Figures are plotted in the following way. Unlike the continuous snake lines plotted for EP in Figure 17 and Figure 18, in Figure 21(a), the black square boxes show the EP for slope failures at which the FOS value reduces less than 1 and the white square boxes show the EP for stable slope cases (FOS equal to or greater than 1) for the series B and C. Similarly, in Figure 21(b), snake lines are plotted with the black square boxes showing the EP for slope failures at which the FOS value reduces less than 1 and the white square boxes show the EP for all stable slope cases (FOS equal to or greater than 1) for the series A and D. This will give an idea about the location of slope failures along the snake lines in a two-dimensional plot. It could be seen that using the designated CL proposed by Matsuura et al. (2013), the failures and stable scenarios during snow melting and thawing seasons are explicitly delineated. The rainfall slope failures are clearly distinguished by the CL proposed by Yano (1990). In comparison to other CLs, the CL3 predicts the slope failure and

stable cases more clearly. Unlike SWI, the EP index does not require a revision in the CL for slope failures occur during snow melting and thawing season. The EP index show the fact that the CL proposed by Matsuura et al. (2013) can be applied to the slope failures in Hokkaido because the original model can consider the effects of snowmelt water on slope failures. Therefore, it is reasonable to apply the CL to slope failures in Hokkaido. On the other hand, the CL for SWI proposed by Nakatsugawa et al. (2015) does not consider the effects of snowmelt water. Therefore, it will be necessary to change the CL for SWI which are discussed in section 6.2.

Revisions of the 60-minute rainfall and SWI relationships

Revisions for the 60-min rainfall and SWI relationships are done by considering the snowmelt water as an input in the calculation of SWI and as shown in Equation 12.

$$S_1(t + \Delta t) = (1 - \beta_1 \Delta t) \times S_1(t) - q_1(t) \times \Delta t + P \quad (12)$$

P is the cumulative hourly precipitation including rainfall and snowmelt water (mm/hr.). In the revised SWI the storage of the tank 1 S_1 includes the contribution of moisture supplied by snowmelt water. The criteria are then applied to the slope failure cases as shown in Figure 22. It could be seen that even after incorporation of the snowmelt water in the calculation, the index does not predict the slope failure. A revision for the threshold line is designated for Hokkaido. In addition, from Figure 17 and 18, it could be seen that the SWI fail to predict the slope failures as the threshold value (CL) is much larger. Similar behaviour has been observed for the Nakayama pass slope failure case (Figure 16) and have been reported by Iwakura et al. (2010) and Nakatsugawa et al (2015) as well. The basic concept of the currently operating Japanese early-warning system (Osanai et al. 2010) explains that the CL for a particular region can be revised if it is necessary. As many researchers have found that the CL designated is not appropriate for the snowy Hokkaido region, in this study the revisions are studied. The critical line designated for Hokkaido is revised based on the slope failure data using the conceptually derived RBFN (Radial Basis

Finite Network) lines as shown in Figure 22. The RBFN is a cluster of slope failure as well as stable data through which JMA delineates the CL. At JMA, the RBFN lines are derived from years and years of occurrences and non-occurrences of slope failures within the preferred area. Of those RBFN lines, the one which could delineate the margin between the failure and stable scenarios is selected as a CL. For all the 448 numbers of slope failures from series B and C and 64 numbers of slope failures from series D, the corresponding SWI were plotted in two-dimensional plane along with many CL as shown in Figure 23(a) and (b) respectively. The failures are identified by checking the FOS is lesser than 1. The stable and failure cases from the series B and C are plotted in Figure 23(a) and from series A and D are plotted in Figure 23(b). These figures are plotted in the same way as the EP index shown in Figure 21(a) and (b). It could be seen that the designated CL does not predict the failures and stable scenarios clearly in Figure 23(a). A clear demarcation between the failures and stable cases are identified at line connecting 30 mm/hr. rainfall and 150 mm SWI. Similar to the procedure followed by JMA (Osanai et al. 2010), a CL line can be delineated between the occurrence and non-occurrences of failures as shown in Figure 23(a). From the possible revisions studied the line with a minimum of 30 mm 60-minute cumulative rainfall and 150 mm SWI is found to be appropriate for the prediction of snowmelt induced soil slope failures. The improvement effect of the prediction by SWI is studied and shown in Table 7. It could be seen from Table 7 that before revising the CL, the rate of successful prediction of slope failures is 0 % for series B and C (thawing and after thawing seasons). After revising the CL, the rate of successful prediction of slope failures is improved to 92.85 % with an unsuccessful prediction rate of 7.15 % for series B and C. Analysing the rate of false predictions (stable cases noted as failures), as shown in Table 8., the rate is 0 % for all the series A, B, C and D before revising the CL. Since there is no prediction made, the possibility of making a false prediction is always zero. Whereas, after revising the CL the false prediction rates increase to 100 % for series A and D and remain 0 % for series B and C. In Figure 23(b) the slope failures and stable cases from series A and D are plotted considering the CL designated for Hokkaido. It

could be seen that most of the slope failures are predicted when considering the existing CL. From this observation, it could be said that the revised CL for SWI is applicable only for the slope failures induced by snowmelt water during thawing and after thawing seasons.

DISCUSSION ON MERITS AND SHORTCOMINGS OF THE PROPOSED METHOD

The merits and demerits of the early warning criteria studied in this paper are summarized here. The Effective Precipitation (EP) index will be useful to predict the slope failures induced by slow soil surface infiltration derived from the snowmelt water. For this purpose, the Effective Precipitation with a 72 hours half-life was found to be appropriate. On the other hand, as seen from the case examples on Typhoon induced sediment disasters in Hokkaido, the CL proposed by Matsuura et al. (2013) for the Effective Precipitation index was found to be exceeding to a large value at all stages as observed from Figure 9. Further, it is found from the numerical simulations that the EP criteria with the CL proposed by Matsuura et al. (2013) considerably over estimates the slope failures for cases in series A and D with a false prediction rate of 100 %. Whereas the CL proposed by Yano (1990) predicts the slope failure and stable cases for the series A and D without a false prediction rate. However, for the cases of slope failures in series B and C (thawing and after thawing seasons), the EP index with the CL proposed by Matsuura et al. (2013) shows 100 % successful prediction rate. Due to this fact, it could be said that the threshold CL for Effective Precipitation index should be changed considering the season. The CL proposed by Matsuura et al. (2013) should be used during snowmelt season and the CL proposed by Yano (1990) should be used during rainy seasons.

The SWI calculated for the case of Nakayama pass slope failure shown in Figure 16 does not predict the slope failure even if the snowmelt water is taken into consideration. The increase in SWI is very small as compared with the increase in Effective Precipitation index when considering the snowmelt water (Figure 18 and Figure 19). Even if the hourly snowmelt water is considered, the SWI does not increase to reach the CL designated for Hokkaido. Whereas, by using the revised CL, the slope failures for most of

the cases in series B and C are predicted with a success rate of 92.85 %. The Nakayama pass slope failure could also be predicted if the revised CL is considered (Figure 17). The 7.15 % of unsuccessful rate comes due to the SWI fail to predict the slope failure in case the amount of rainfall is very low. Whereas, a 100 % success rate is achieved by the EP index predicting all the numerical slope failures and case examples during the snowmelt season precisely. On the other hand, the revised CL for SWI considerably over estimates the slope failures for cases in series A and D with a false prediction rate of 100 %. With the currently available CL for Hokkaido, the slope failures and stable cases are delineated with more accuracy as shown in Figure 23(b).

It could be suggested that, for the prediction of snowmelt induced soil slope failures, the Effective Precipitation index would be appropriate rather than the Soil Water Index. Whereas, the Soil Water Index would be appropriate to predict the failures induced by heavy rainfall i.e. Typhoon etc. Since the objective of this study is to find some criteria for the prediction of snowmelt induced soil slope failures in cold regions, the use of Effective Precipitation (EP) index is recommended. On the other hand, from these detailed studies of early warning criteria, it is also significant to note the advantages of performing numerical simulations to revise the CLs for EP and SWI. Based on the studies performed, it has been found that numerical simulations can be reasonably used to set the CL for both snowmelt and rainfall induced slope failures since the results of stable and slope failure cases agree well with the existing CLs.

CONCLUSIONS

This paper evaluates the applicability of Japanese early warning criteria Soil water index (SWI) and Effective Rainfall index (ER) for the prediction of snowmelt induced soil slope failures in Hokkaido, Japan. Through adopting a numerical analysis approach and considering the construction of a risk assessment method for slope disasters in snowy cold areas, various scenarios of conceptual soil slope failures are studied under different magnitudes of rainfall and snowmelt water. As a result, a revision for the SWI and a new early warning criterion Effective Precipitation (EP) index is introduced. An empirical

equation to estimate the hourly snowmelt water is used. Snowmelt water is explicitly considered in both SWI and EP. It is found that the revised SWI and new failure criterion EP perform well for the prediction of snowmelt induced soil slope failures in Hokkaido, Japan. Following findings can be outlined from this study.

- Consideration of snowmelt water improves the prediction using SWI, provided a revision of Critical Line for Hokkaido is made. The revisions for the criteria are studied and an hourly threshold rainfall + snowmelt value 30 mm/hr. is proposed and for SWI a value of 150 mm is recommended. The suggested revised CL for the SWI is applicable only for the slope failures occur during snow melting and thawing and after thawing seasons. For the slope failure occurring during rainy seasons the existing CL for Hokkaido is found appropriate.
- The proposed Effective Precipitation (EP) index performs well if snowmelt water is included in the calculation. As compared with other half-lives (6 hours and 24 hours), the 72-hour half-life provides a reasonable estimation of the soil moisture. The EP with 1.5 hours half-life and 72 hours half-life considers both the effect of high rainfall amount for short duration and small rainfall amount for long duration through which the short-term and long-term infiltration effects of soil moisture can be considered as seen from the comparative studies. The snowmelt water can also be precisely considered in these criteria.
- As compared with the SWI using revised CL, the proposed Effective Precipitation (EP) index predicts the snowmelt as well as rainfall induced soil slope failures with higher accuracy provided different CLs are used in accordance with the respective types of slopes failure. The different critical lines presented for snowmelt as well as rainfall induced slope failures predicts the failures and stable scenarios more accurately than the SWI.

- The results of numerical simulations (stable cases and slope failures) performed in this study agree well with the existing CL of EP and SWI. Numerical simulations can be practically used to set the CL for both snowmelt and rainfall induced soil slope failures.

In the context of climate change, geohazards in high latitude northern cold regions are ever increasing. In this paper, based on the recent abnormal weather and considering the progress of climate change in the future, based on the rainfall history of sediment-related disasters that occurred in the past and assuming cases where it will be difficult to set the sediment-related disaster risk criterion line (CL: Critical Line), the amount of snowmelt water and rainfall is considered to construct a slope disaster risk assessment method for snowy cold climate areas using numerical analysis as a tool. It has been shown possible to set the criteria for sediment-related disaster warning information in snowy cold regions considering rainfall and snowmelt water. Therefore, this study has proved and opened an approach to evaluate the risk of potential sediment-related disasters that can also be applied regionally for wide area disaster risk assessments considering factors such as rainfall, snowmelt water and freezing index into account.

ACKNOWLEDGEMENTS

We gratefully acknowledge the Sapporo Road Office, Bureau of Hokkaido Development and Docon Co., Ltd. for their surveyed data and comments. This research was supported in part by Grant-in-Aids for Scientific Research (A) (16H02360) from Japan Society for the Promotion of Science (JSPS) KAKENHI. The financial support provided by the MEXT (Ministry of Education, Culture, Sports, Science and Technology in Japan) scholarship is also gratefully acknowledged.

REFERENCES

Abe, O. and Shimizu, M. 2009. Equivalent snow density to estimate snow load in extremely heavy snow areas, *Journal of the Japanese Society of Snow and Ice*, 66(1), 11-16. (In Japanese). <https://doi.org/10.5331/seppyo.66.11>

- Berris, S. N. and Harr, R. D. 1987. Comparative snow accumulation and melt during rainfall in forested and clear-cut plots in the western Cascades of Oregon. *Water Resources Research*, 23(1), 135-142.
- Hokkaido Regional Development Bureau., 2014. Report on slope disaster, recovery and survey design. Route No 230 Sapporo general national highway. Sapporo Development and Construction Department, Sapporo (In Japanese).
- Ishida, K., Minami., N. Yamada, T., Ishida, T., Kato, N. and Yoshikawa, M. 2000. A Study for Determining the Warning and Evacuation Criteria of Snowmelt - induced Debris Flow. *Journal of the Japan Society of Erosion Control Engineering*. 52 (5), 46-51. (in Japanese with English abstract).
- Ishikawa, T., Tokoro, T. and Seiichi, M., 2015. Geohazard at volcanic soil slope in cold regions and its influencing factors. *Japanese Geotech. Soc. Spec. Publ.* 1, 1–20. doi:10.3208/jgssp.KEY-1
- Iwakura, T., Takayoshi, K., Otani, H., Tanimoto, K., Tokioka, S. and Watanabe, T. 2010. Study of warning and evacuation standard-setting approach to the sediment-related disasters that occur in the snowmelt season. 59th Annual Meeting of the Society of Erosion Control Research. Paper 229. (In Japanese).
- Iwata, Y., Nemoto, M., Hasegawa, S., Yanai, Y., Kuwao, K., Hirota, T., 2011. Influence of rain, air temperature, and snow cover on subsequent spring-snowmelt infiltration into thin frozen soil layer in northern Japan. *J. Hydrol.* 401, 165–176.
- Japanese Geotechnical Society., 2017. The final report of ground disaster investigation report due to heavy rain in Hokkaido during August 2016. (in Japanese)
https://www.jiban.or.jp/wp-content/uploads/2017/08/final_report_ver0.12s.pdf
- Japan Meteorological Agency (JMA) 2012. Soil Water Index, (in Japanese), Date accessed: August 20th, 2012. <http://www.jma.go.jp/jma/kishou/known/bosai/dojoshisu.html>
- Japan Meteorological Agency (JMA) 2016. Talas Soil Water Index, http://www.jma.go.jp/jma/en/News/Talas_soil_water_index.html. Date accessed: December 15th, 2016.

- Kawamura, S., Miura, S. and Matsumura, S., 2016. Stability evaluation of full-scale embankment constructed by volcanic soil in cold regions. *Japanese Geotech. Soc. Spec. Publ.* 2, 971–976. doi:10.3208/jgssp.JPN-063
- Kondo J., and Yamazaki T. 1990. A Prediction Model for Snowmelt, Snow Surface Temperature and Freezing Depth using a Heat Balance Method, *J. Appl. Meteor.*, 29, 375–384.
- Komarov, V.D., Makarova, T.T., 1973. Effect of the ice content, temperature, cementation, and freezing depth of the soil on meltwater infiltration in a basin. *Soviet Hydrology: Selected Papers* 3, 243–249
- Matsumura, S., 2014. Laboratory and in-situ studies on mechanical properties of volcanic soil embankment in cold region. PhD Thesis, Graduate School of Engineering, Hokkaido University, Japan. <http://hdl.handle.net/2115/55535> (accessed 01.02.2015)
- Matsuura, S., 1998. Difficulties in Predicting Snow-induced Landslides. *Journal of Japan Landslide Society* 34 (4), 39-46. (In Japanese with English abstract)
- Matsuura, S., 2000. Fluctuations of pore-water pressure in a landslide in a heavy snow district. *Journal of Japan Landslide Society* 37 (2), 10-19.
- Matsuura, S., Matsuyama, K., Asano, S., Okamoto, T. and Takeuchi, Y., 2005. Fluctuation of the seasonal snowpack in a mountainous area of the heavy-snow district in the warm-temperate zone of Japan. *J. Glaciol.* 51, 547–554. doi:10.3189/172756505781829052
- Matsuura, S., Asano, S. and Okamoto, T., 2008. Relationship between rain and/or meltwater, pore-water pressure and displacement of a reactivated landslide. *Eng. Geol.* 101, 49–59. doi:10.1016/j.enggeo.2008.03.007
- Matsuura, S., Okamoto, T., Asano, S. and Matsuyama, K., 2013. Characteristics of meltwater and/or rainfall regime in a snowy region and its effect on sediment-related disasters. *Bull. Eng. Geol. Environ.* 72, 119–129. doi:10.1007/s10064-012-0456-1
- Motoyama, H., 1990. Simulation of seasonal snow cover based on air temperature and precipitation. *J. Appl. Meteorol.* 29. 1104-1110.
- Nakatsugawa, M., Usutani, T. and Miyazaki, T., 2015. Risk assessment of sediment disaster based on watershed-wide hydrologic processes. E-proceeding of the 36th IAHR World Congress. <https://www.iahr.org>.
- Okada K (2001) Soil water index. *Sokkoujihou* No.69, 5(5):67-100 (in Japanese)
- Okimura, T. and Ichikawa, R., 1985. A prediction method for surface failures by movements of infiltrated water in a surface soil layer. *Nat. disaster Sci.* 7, 41–51.

- Osanai, N., Shimizu, T., Kuramoto, K., Kojima, S., and Noro, T., 2010. Japanese early-warning for debris flows and slope failures using rainfall indices with Radial Basis Function Network. *Landslides*. 7, 325–338. doi:10.1007/s10346-010-0229-5
- Riley, J.P., Chadwick, D.G. and Eggleston, K.O., 1969. Snowmelt Simulation. Reports. Paper 122. http://digitalcommons.usu.edu/water_rep/122.
- Senoo, K., Haraguchi, K., Kikui, T. and Yoshida, S., 2001. On the theme and improvement of standard rainfall for warning and evacuation from sediment disasters. *Journal of the Japan Society of Erosion Control Engineering*, Vol. 53, No. 6, p. 37-44. (in Japanese with English abstract)
- Siva Subramanian, S., Ishikawa, T., Yokohama, S. and Tokoro, T., 2015. Numerical simulation of volcanic soil slope failure under coupled freeze-thaw and rainfall infiltration effects. *Japanese Geotech. Soc. Spec. Publ.* 1, 5–10. doi: <http://doi.org/10.3208/jgssp.JPN-23>
- Siva Subramanian, S., Ishikawa, T. and Tokoro, T., 2017. Stability assessment approach for soil slopes in seasonal cold regions. *Engineering Geology*. doi: <http://doi.org/10.1016/j.enggeo.2017.03.008>
- Singh, P., Spitzbart, G., Hubl, H. and Weinmeister, H. W., 1997. Hydrological response of snowpack under rain-on-snow events: a field study, *Journal of Hydrology*, 202(1-4), 1-20.
- Tereda, H. and Nakaya, H., 2001. Operating methods of critical rainfall for warning and evacuation from sediment-related disasters. Technical Note of National Institute for Land and Infrastructure Management. No. 5. Ministry of Land, Infrastructure and Transport, Japan (in Japanese).
- Williams, M.W., Cline, D., Hartman, M. and Bardsley, T., 1999. Data for snowmelt model development, calibration, and verification at an alpine site, Colorado Front Range, *Water Resources Research*, 35-10, 3205-3209
- Yano, K., 1990. Study of the method for setting standard rainfall of debris flow by the reform of antecedent rain. *Japan Society of Erosion Control Engineering* 43(4), 3-13 (in Japanese with English abstract).

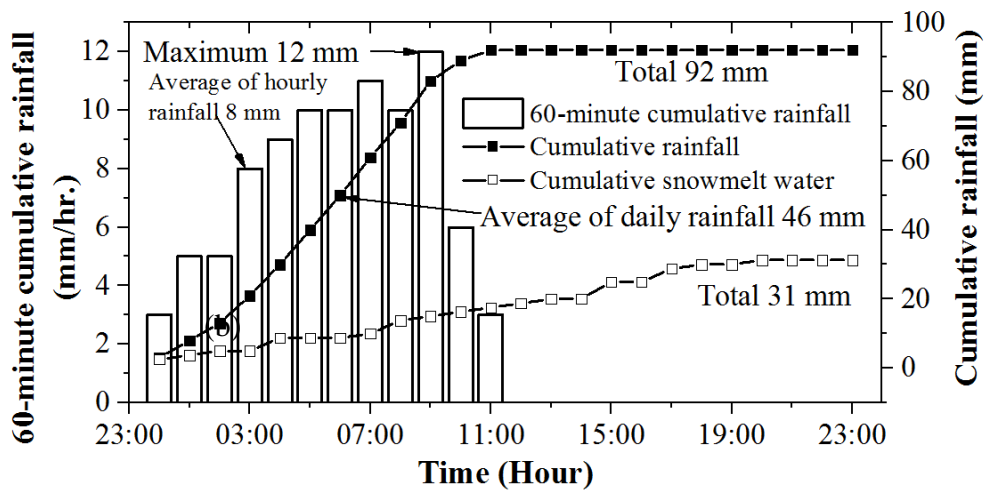
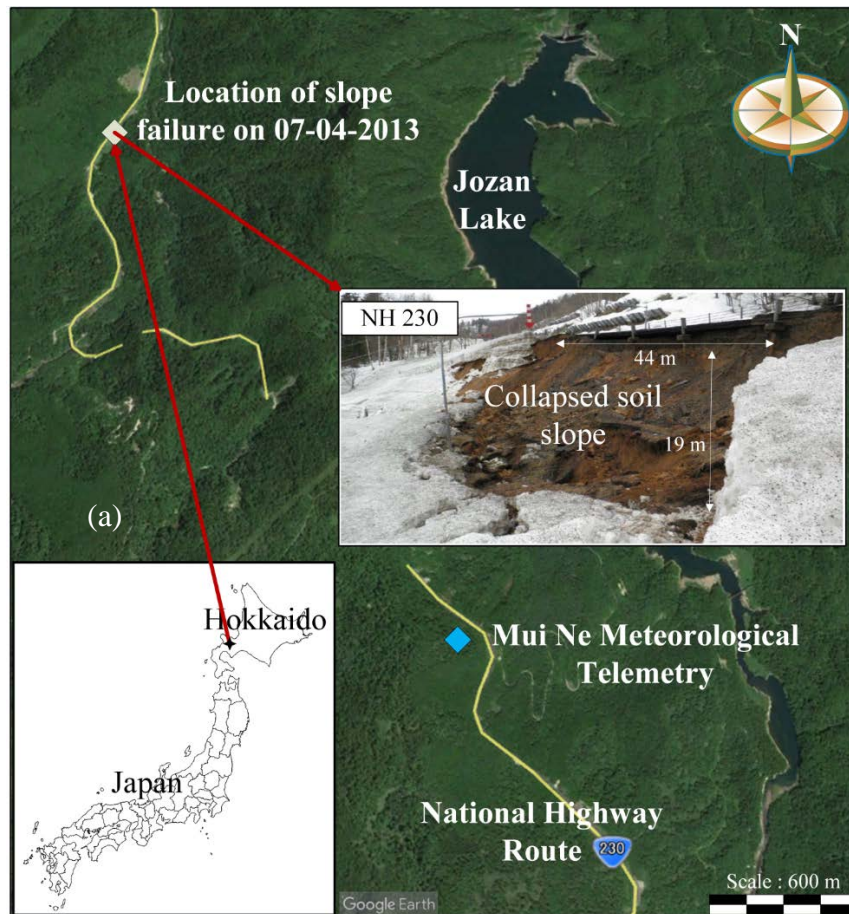


Figure. 1 (a) Locations of slope failure and meteorological telemetry along National Highway Route 230 and panoramic view of the slope failure (adapted from Hokkaido regional development bureau, 2014) and (b) Rainfall and snowmelt recorded on 07-04-2013 at Mui Ne meteorological telemetry



Figure 2 Typhoon affected disasters in Hokkaido during the month of August 2016.

Many occurrences of small to large sediment disasters along Doto Expressway and National Highway routes (Japanese Geotechnical Society, 2017)

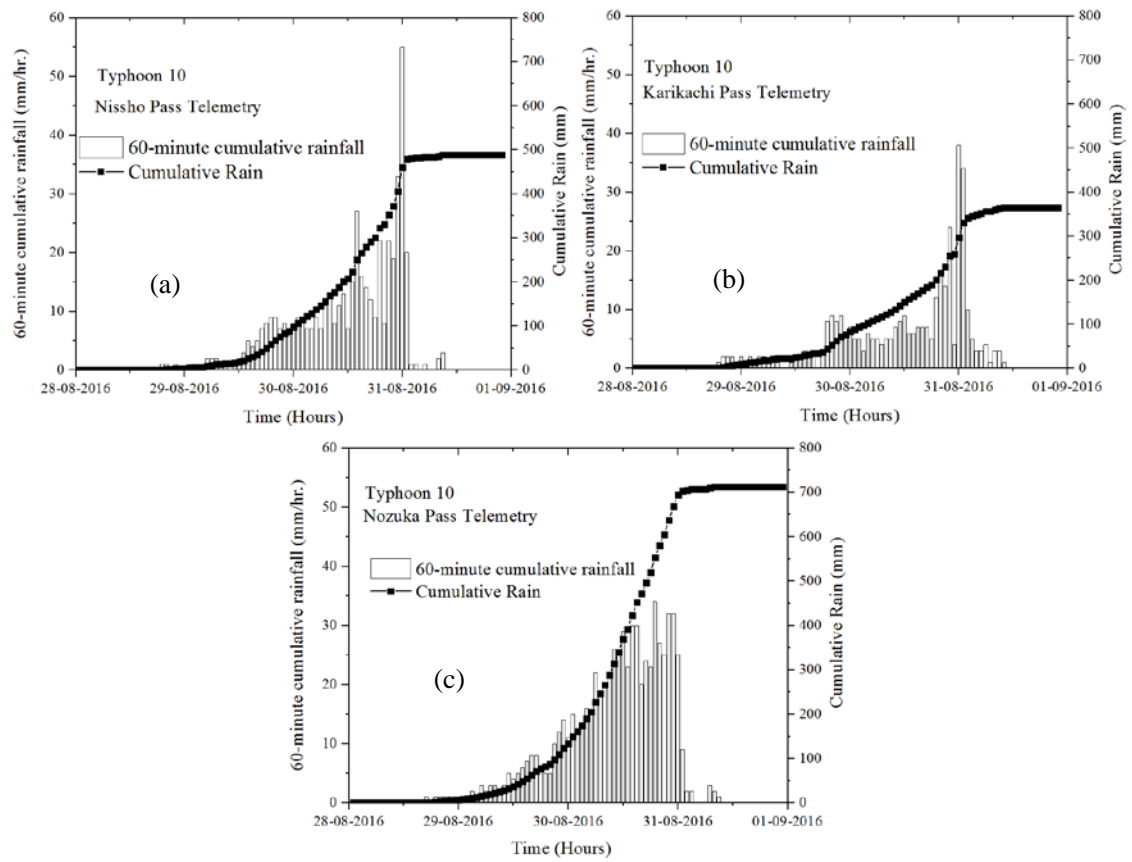


Figure 3 Rainfall recorded during typhoon at (a) Nissho pass meteorological telemetry (b) Karikachi pass meteorological telemetry and (c) Nozuka pass meteorological telemetry

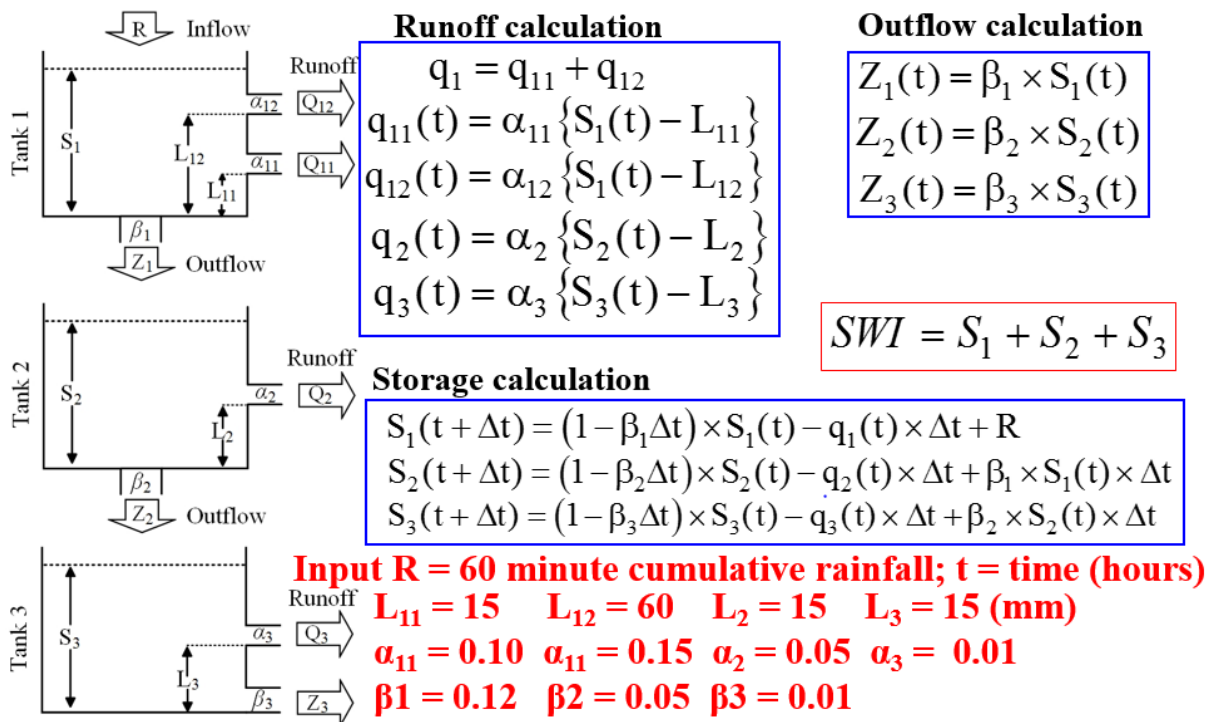


Figure 4 Three-layer tank model for Soil Water Index (adapted from Okada, 2001)

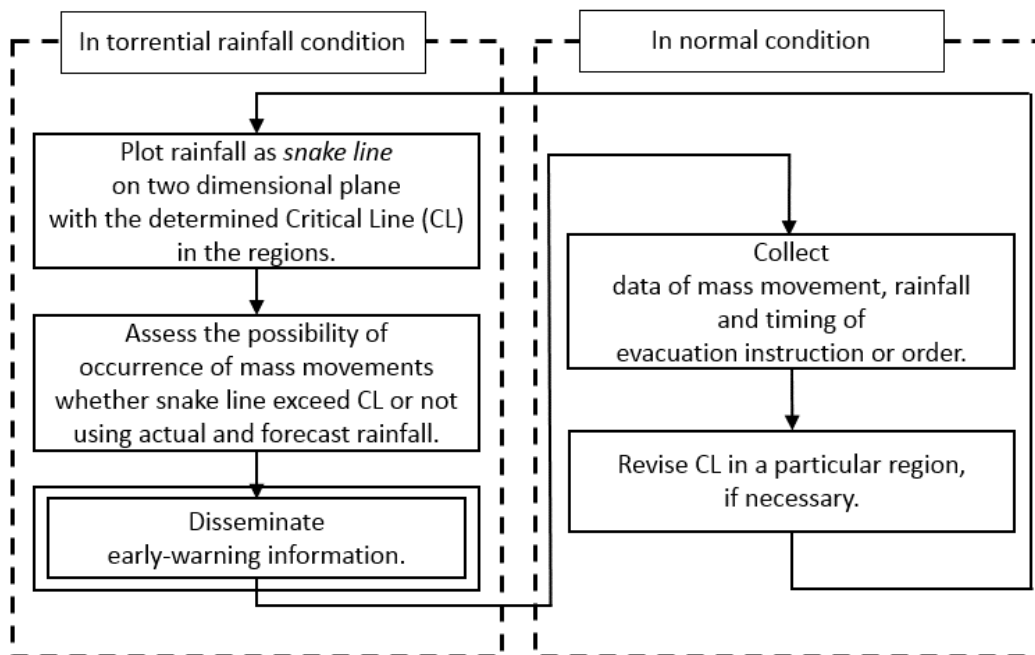


Figure 5 Basic concept of the currently operating Japanese early-warning system (adapted from

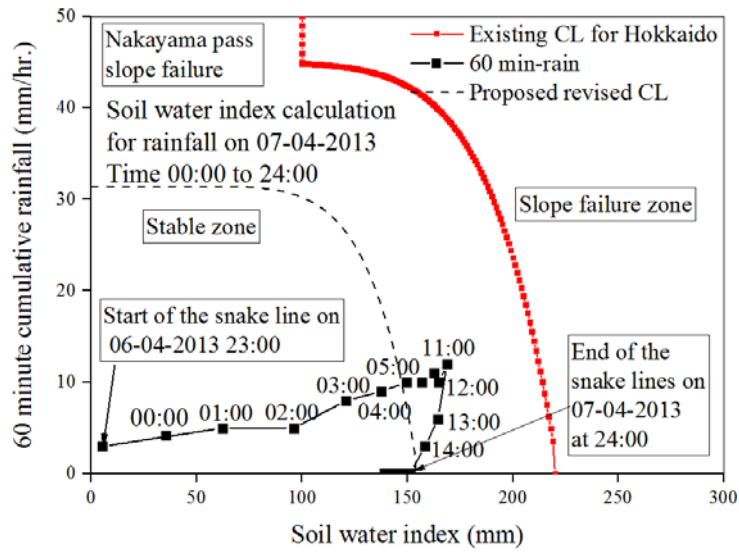


Figure 6 60-minute cumulative rainfall and Soil Water Index relationships (SWI) for Slope failure on April 2013 along National Highway Route 230

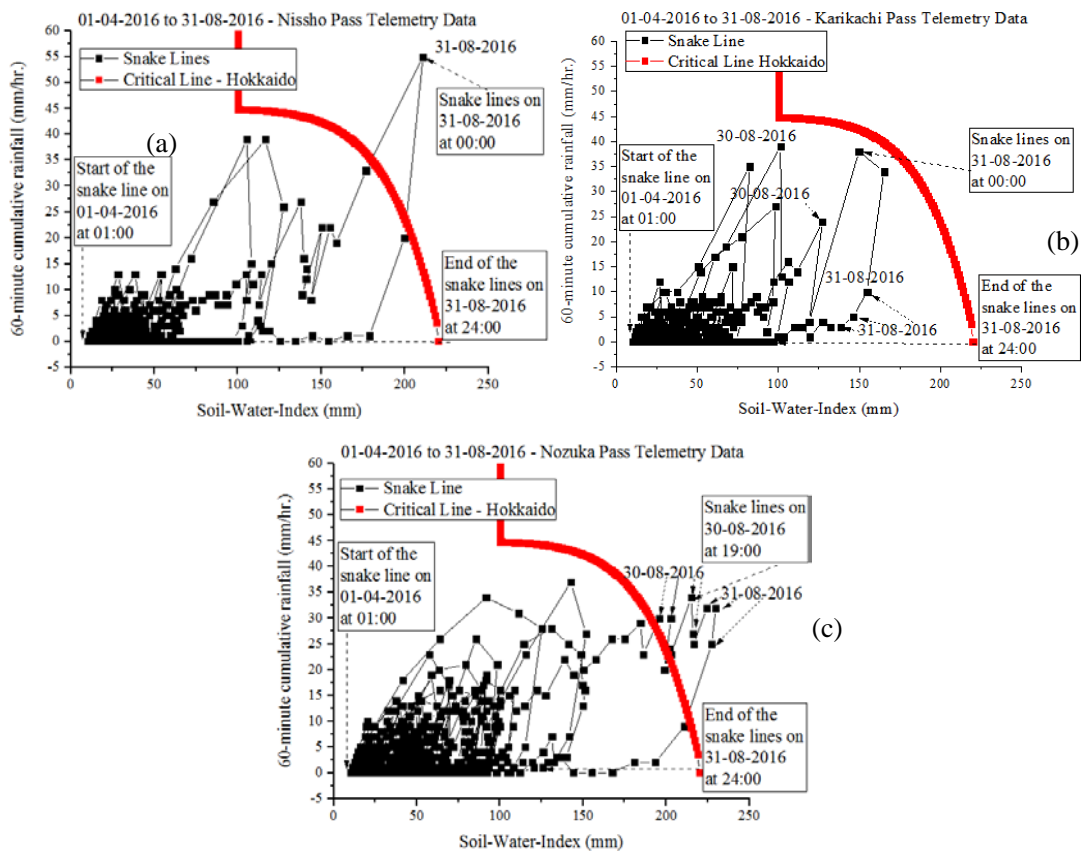


Figure 7 60-minute cumulative rainfall and Soil Water Index relationships (SWI) for data collected from (a) Nissho pass, (b) Karikachi pass and (c) Nozuka pass telemetries

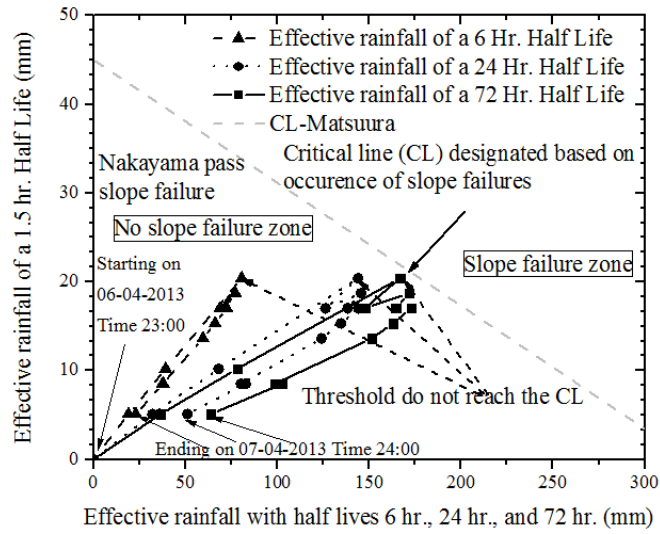


Figure 8 Plot of Effective rainfall index with half-life 1.5 hours (y axis) and half-lives 6 Hours, 24 Hours and 72 hours in (x axis) for the case of Nakayama pass slope failure.

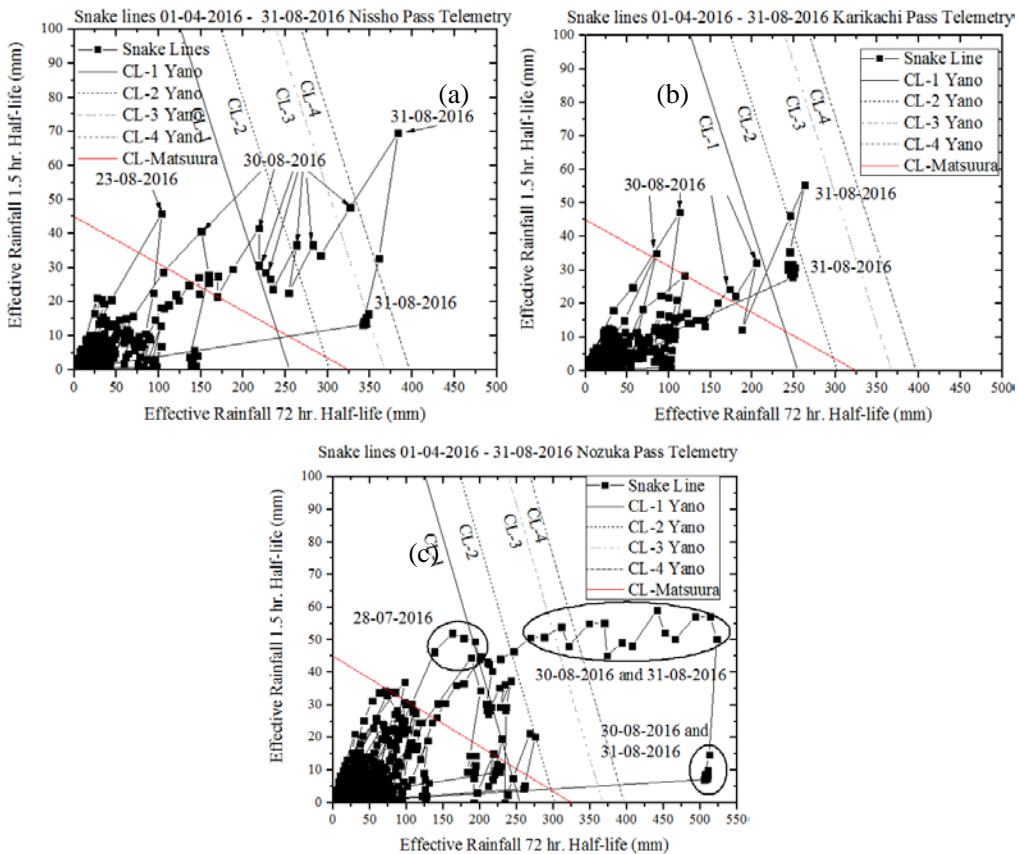


Figure 9 Snake lines plotted for the data recorded from (a) Nissho Pass, (b) Karikachi Pass and (c) Nozuka Pass Telemetries

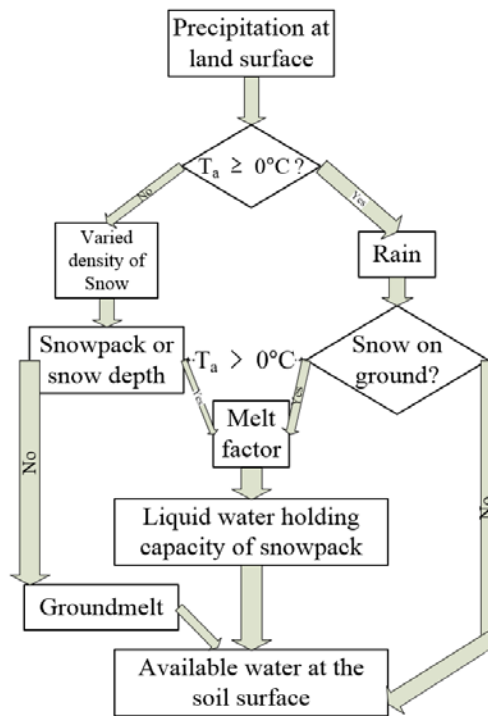


Figure 10 Model to estimate hourly snowmelt water (after Riley et al. 1969)

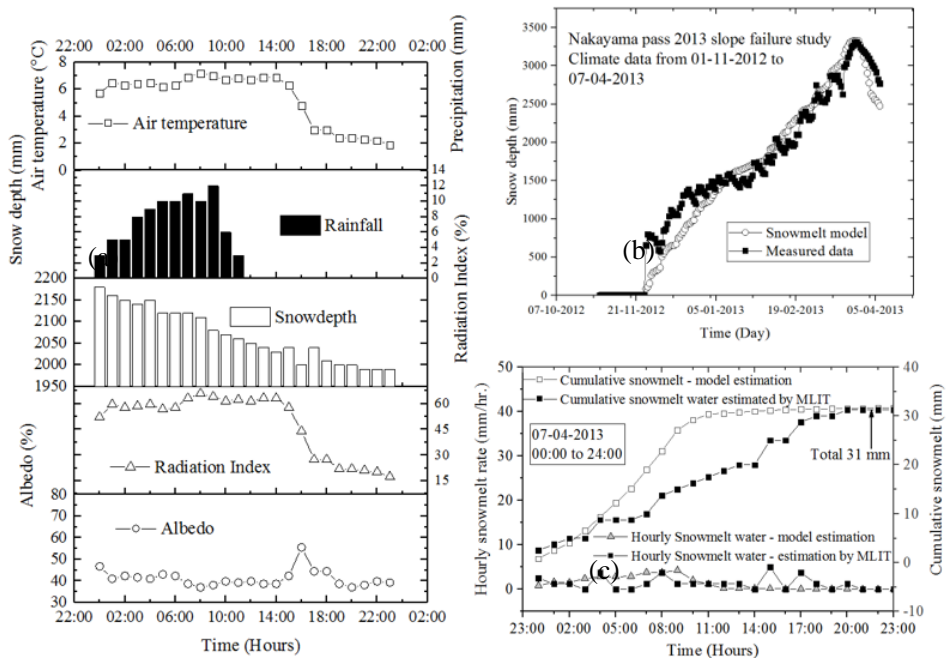


Figure 11 Estimation of snowmelt water using snowmelt model (a) climate data for Nakayama pass slope failure on 07-04-2013, (b) comparison of estimated and measured change in snow depth and (c) comparison of estimated snowmelt water on 07-04-2013.

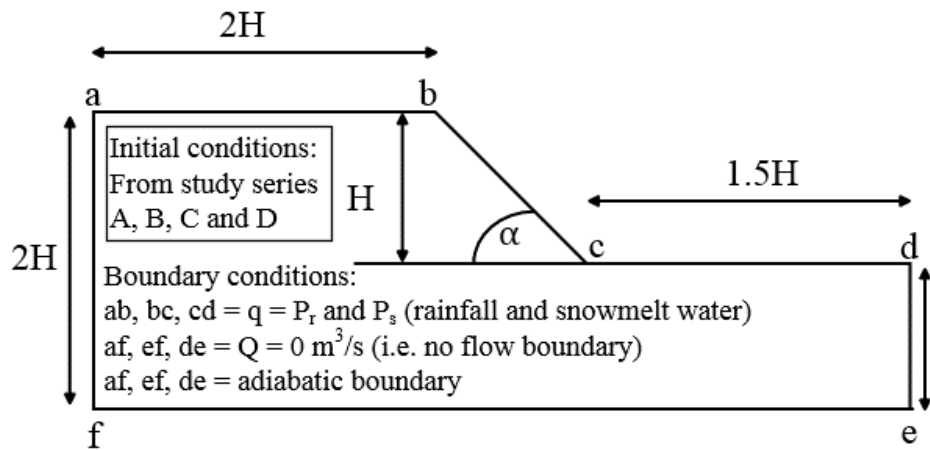


Figure 12 Slope geometry and boundary conditions for homogeneous soil slope used in parametric studies

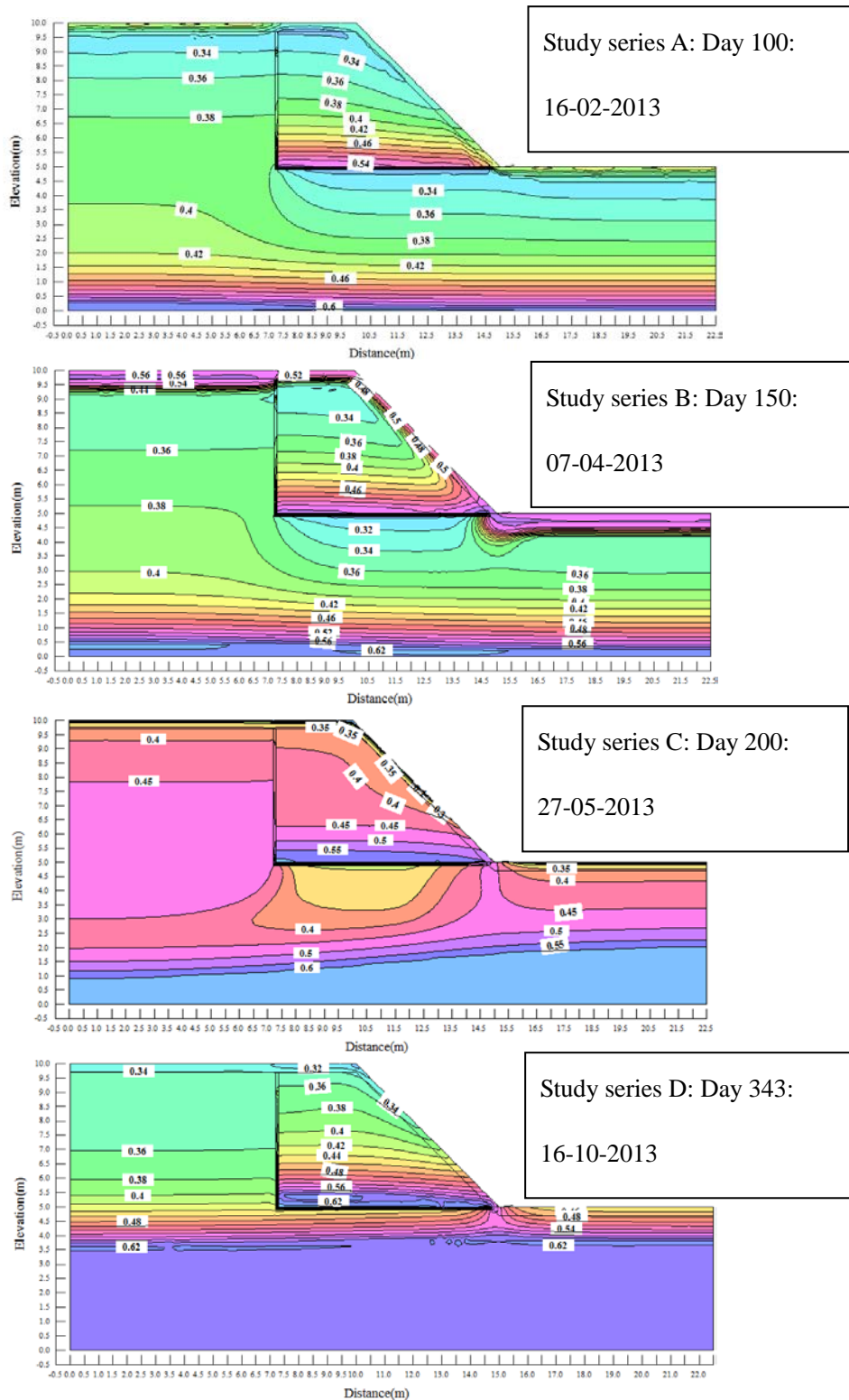


Figure 13 Initial volumetric water content (m^3/m^3) distributions during four different seasons

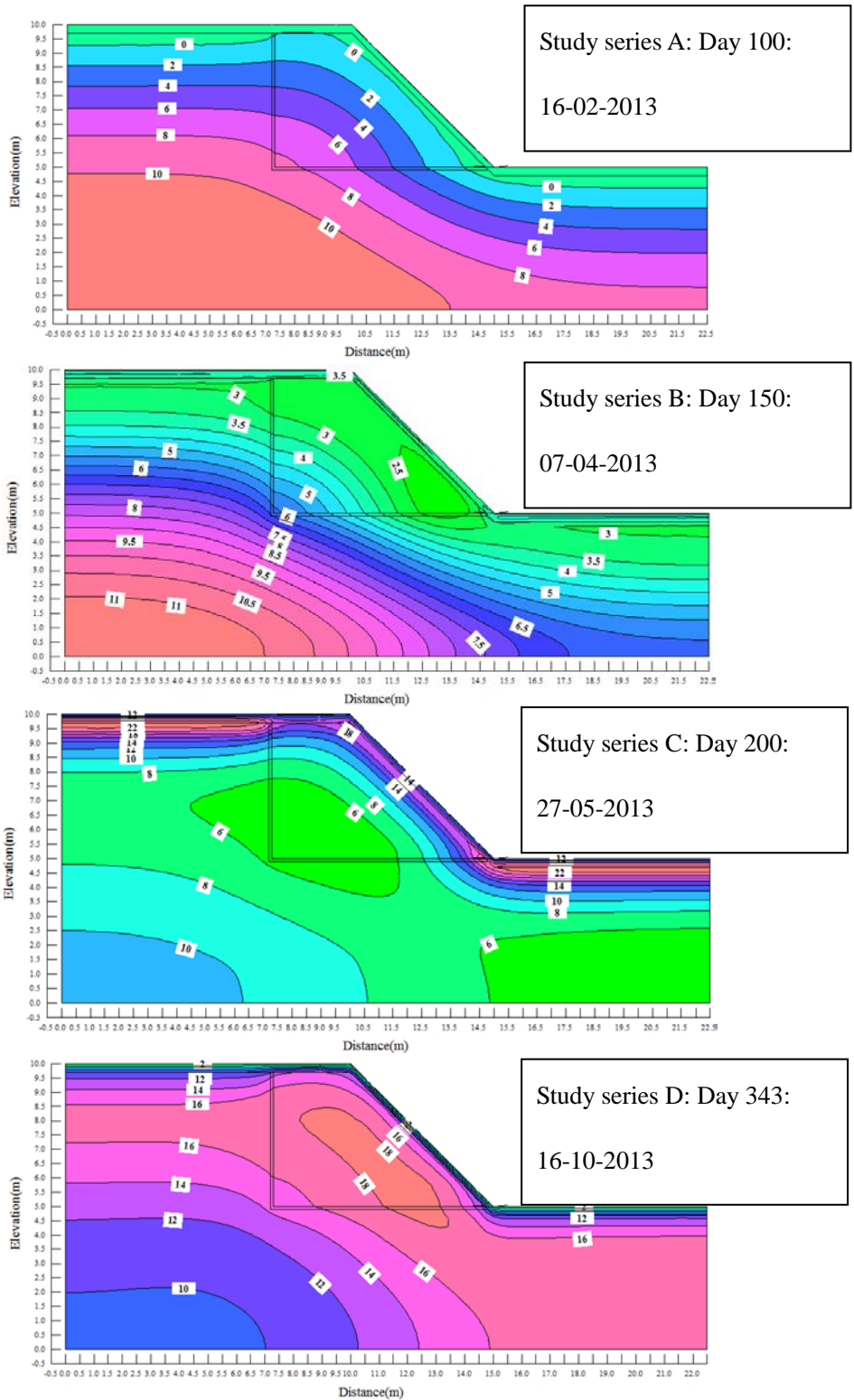


Figure 14 Initial temperature (°C) distributions during four different seasons

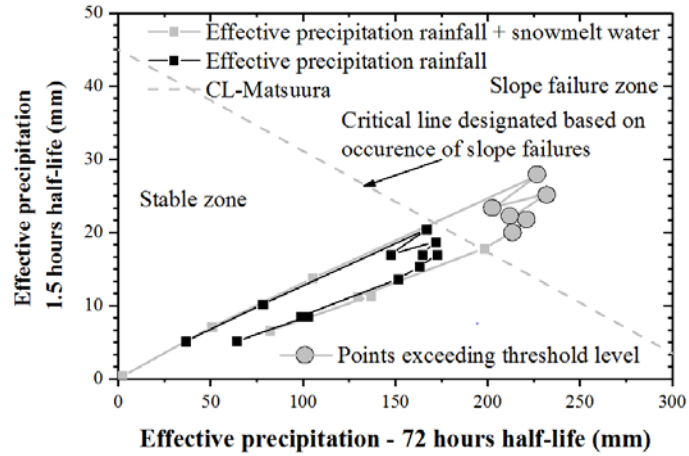


Figure 15 Possible revisions of the Effective rainfall index with snowmelt water/ Effective precipitation index

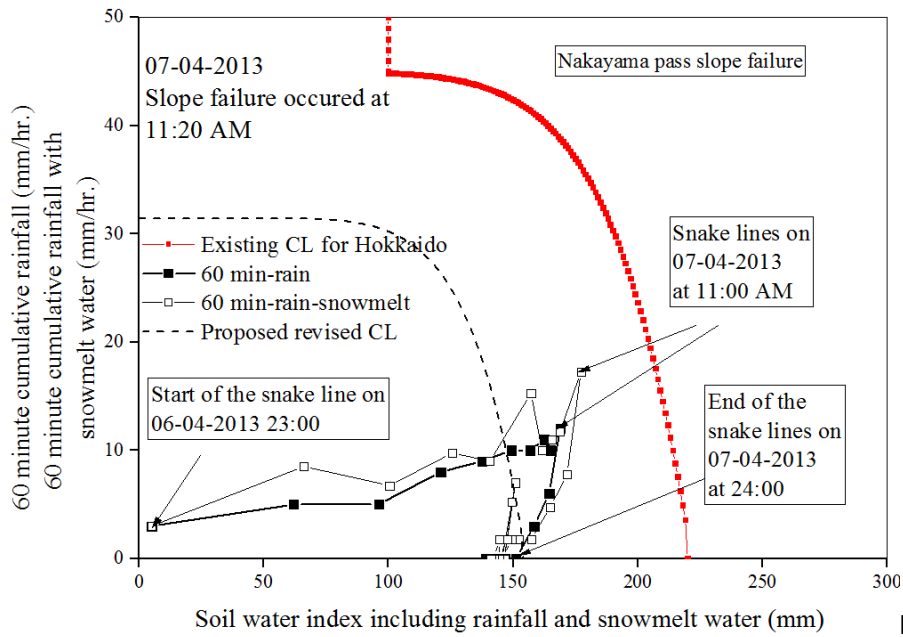


Figure 16 Prediction of Nakayama pass slope failure with consideration of snowmelt water using SWI

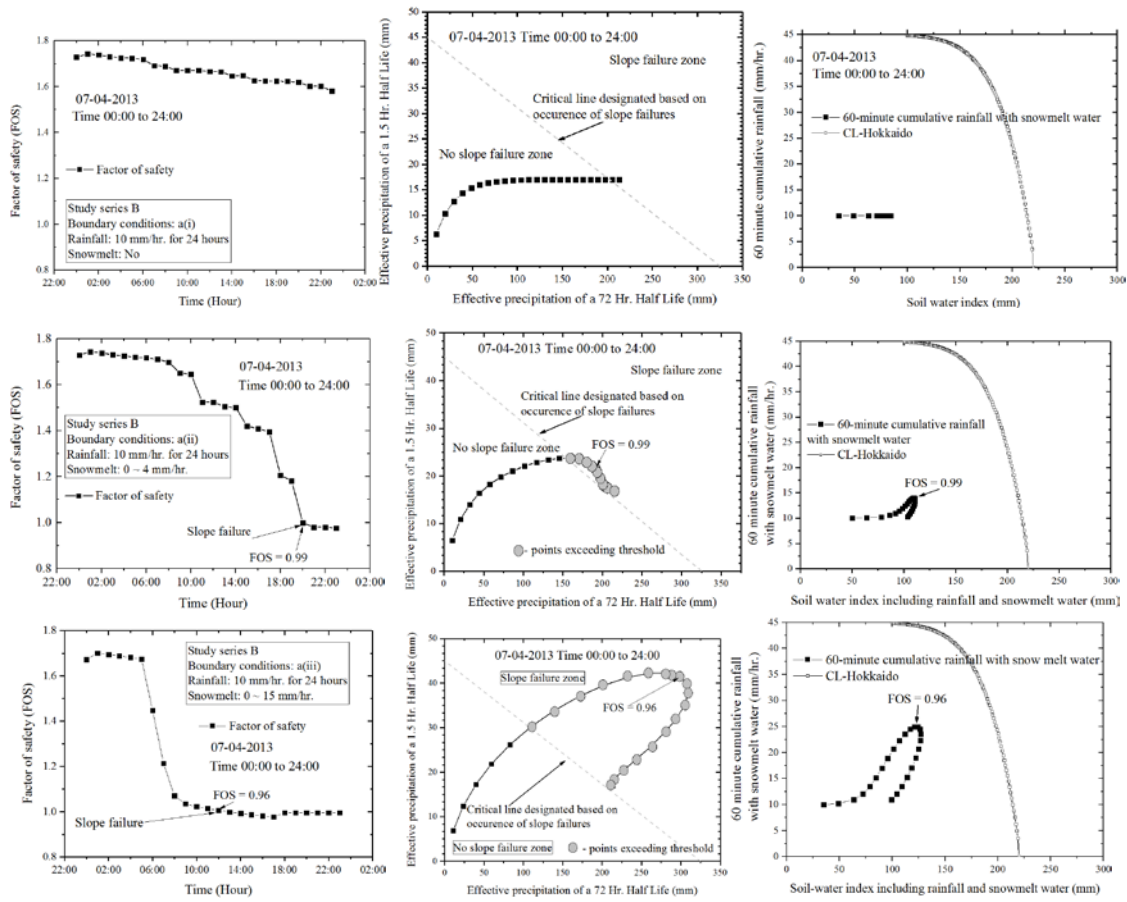


Figure 17 Factor of safety, Effective Precipitation index and Soil Water Index for study series B

with 45° slope angle, 5 m slope height, 10 mm/hr. rainfall with two different snowmelt rates

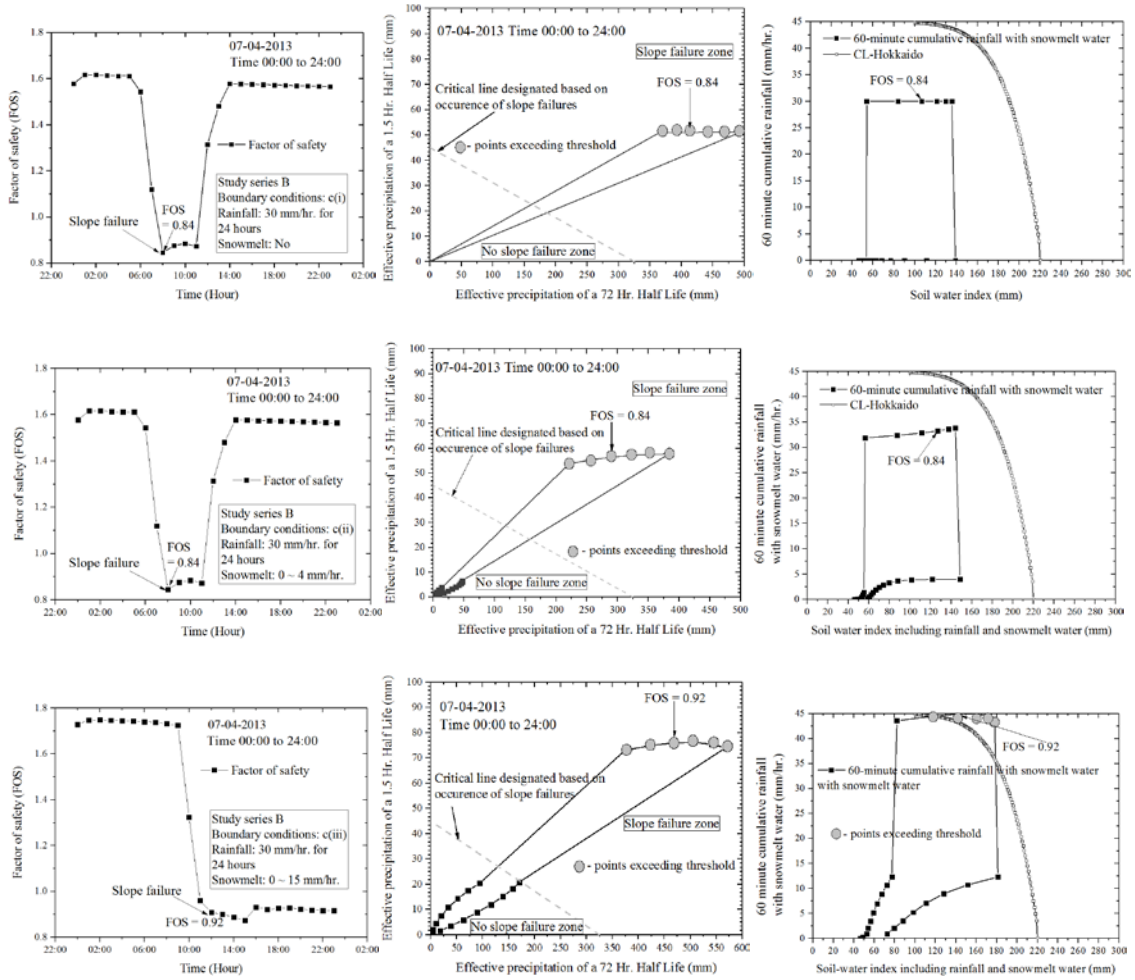


Figure 18 Factor of safety, Effective Precipitation index and Soil Water Index with 45° slope angle, 5 m slope height, 30 mm/hr. rainfall with two different snowmelt rates

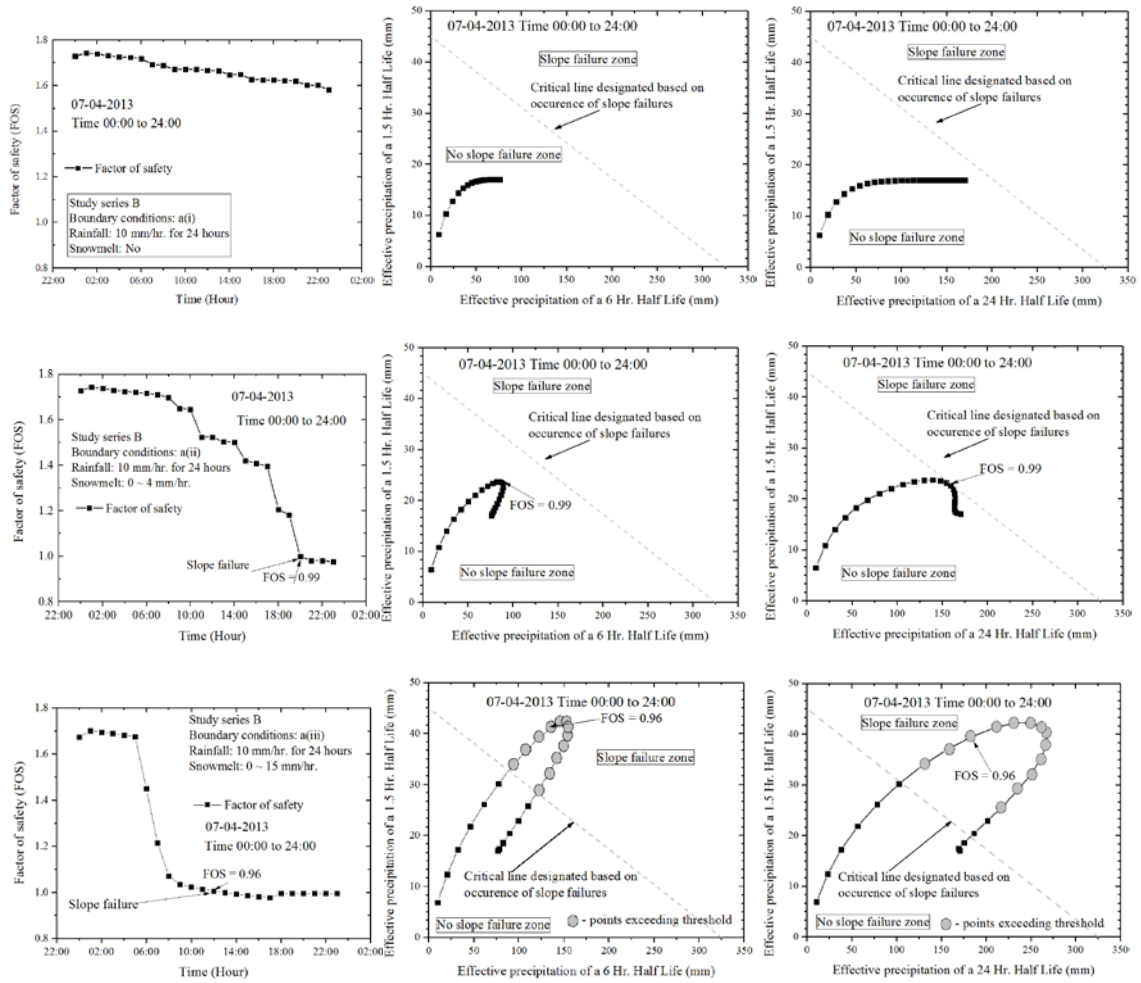


Figure 19 Comparison of Factor of safety, Effective Precipitation index 6 hours half-life and 24 hours half-life for study series B with 45° slope angle, 5 m slope height, 10 mm/hr. rainfall with two different snowmelt rates

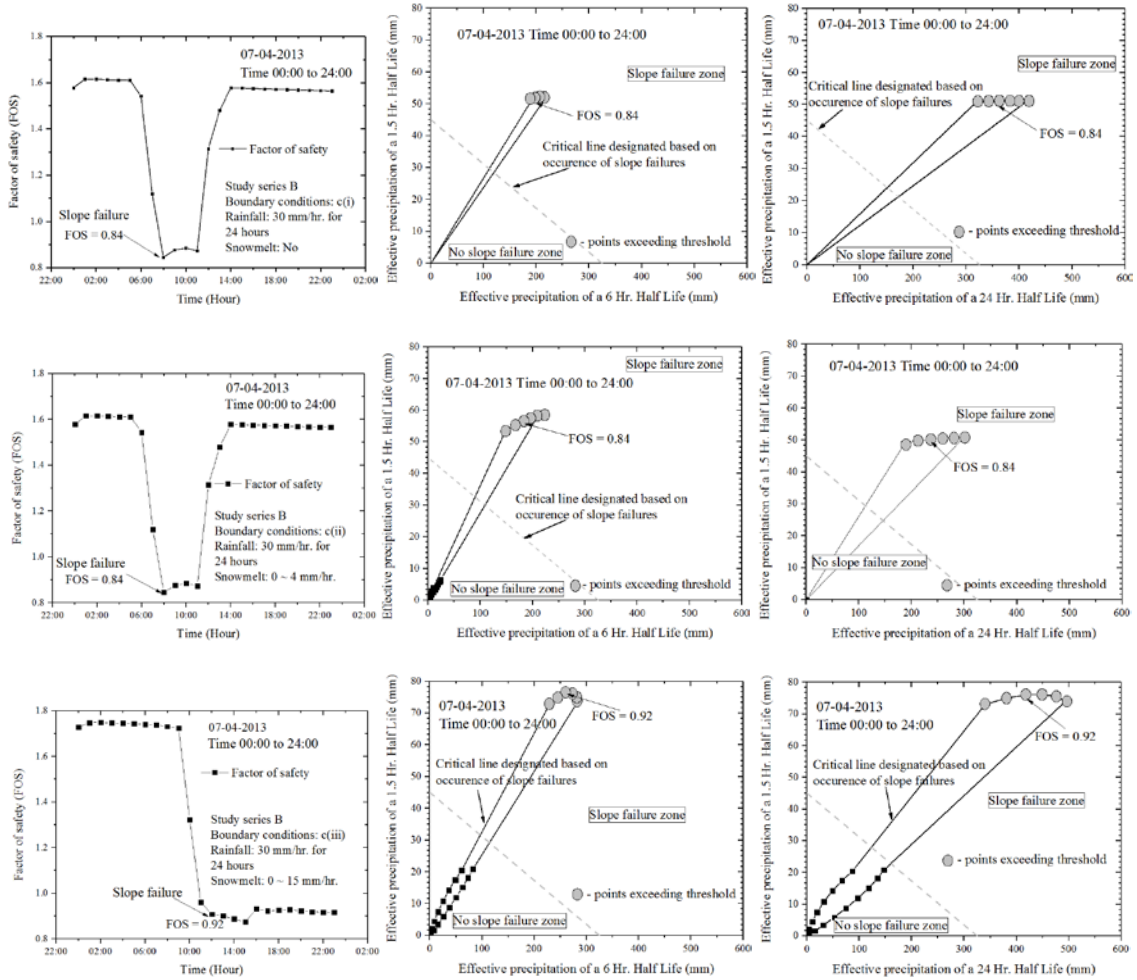


Figure 20 Comparison of Factor of safety, Effective Precipitation index 6 hours half-life and 24 hours half-life for study series B with 45° slope angle, 5 m slope height, 30 mm/hr. rainfall with two different snowmelt rates

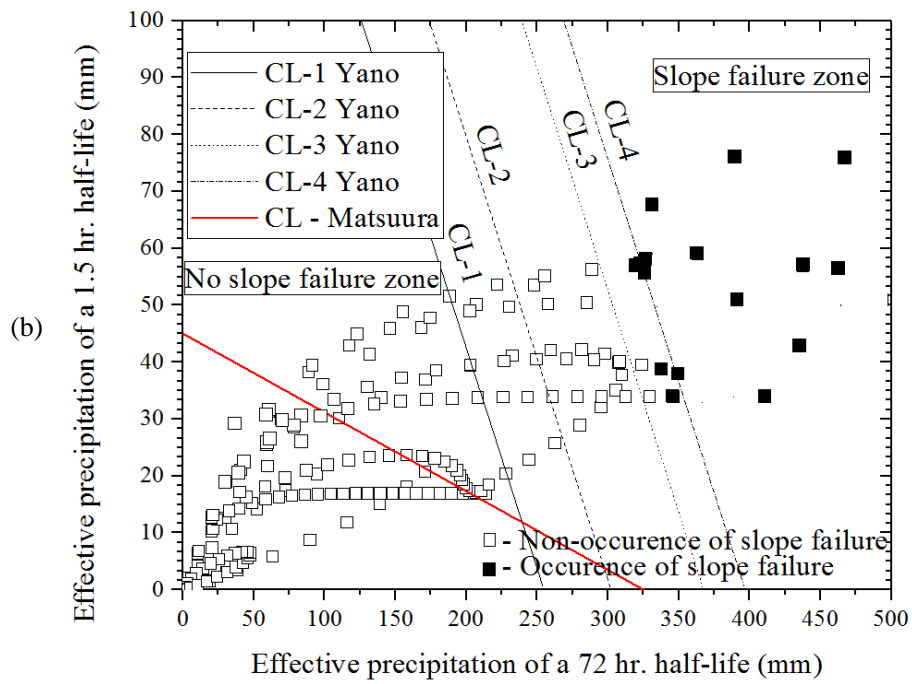
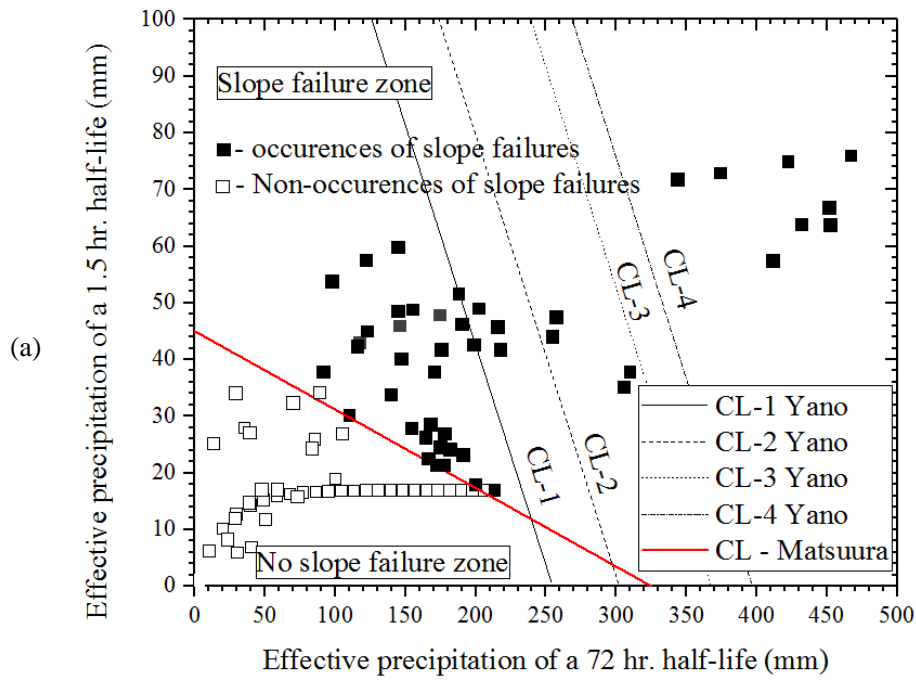


Figure 21 Plots of all slope failures and stable cases using Effective Precipitation index with half-lives 1.5 hours and 72 hours (a) series B and C, (b) series A and D.

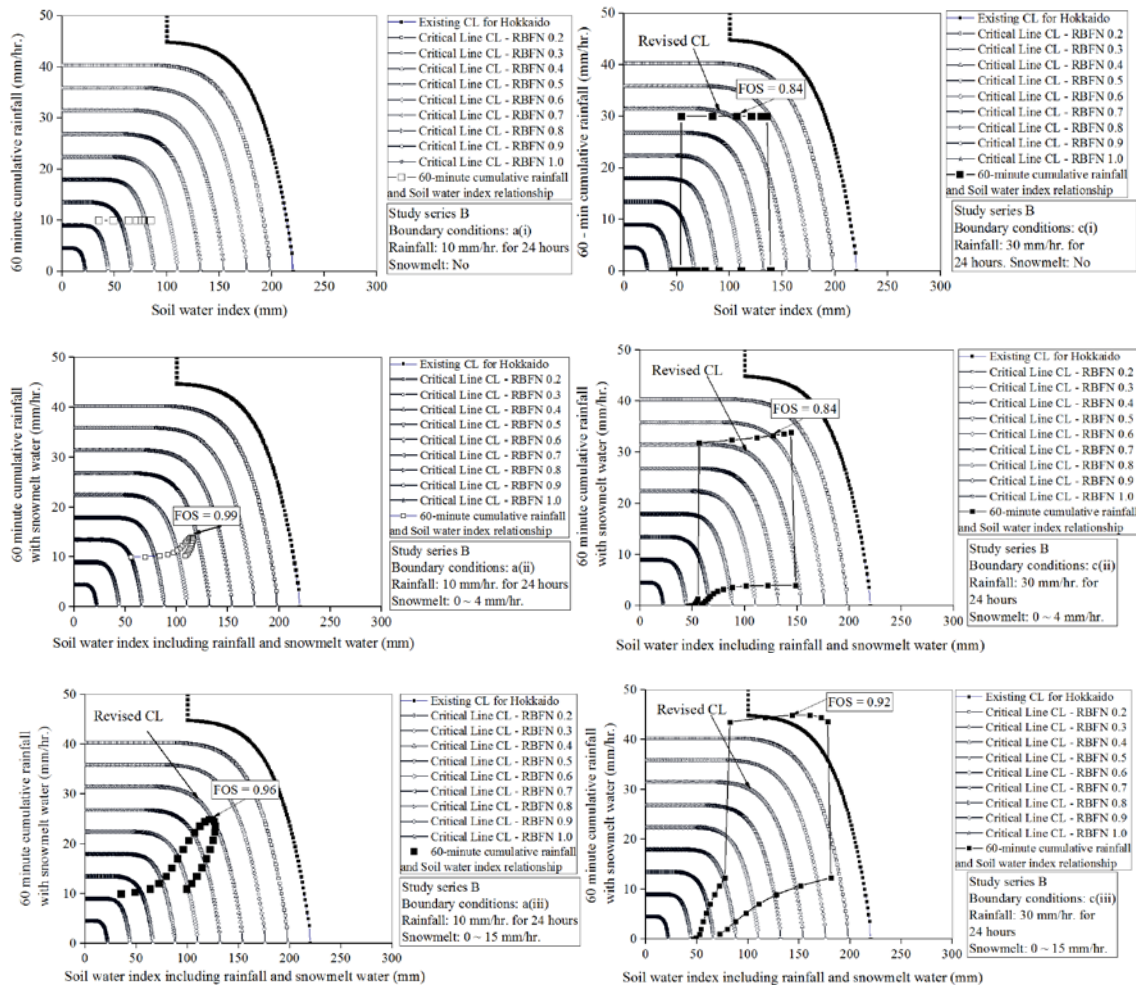


Figure 22 Revision of CL for SWI based on occurrence and non-occurrence of slope failures using data from study series B with 45° slope angle, 5 m slope height, 10 mm/hr. and 30 mm/hr. rainfall with two different snowmelt rates

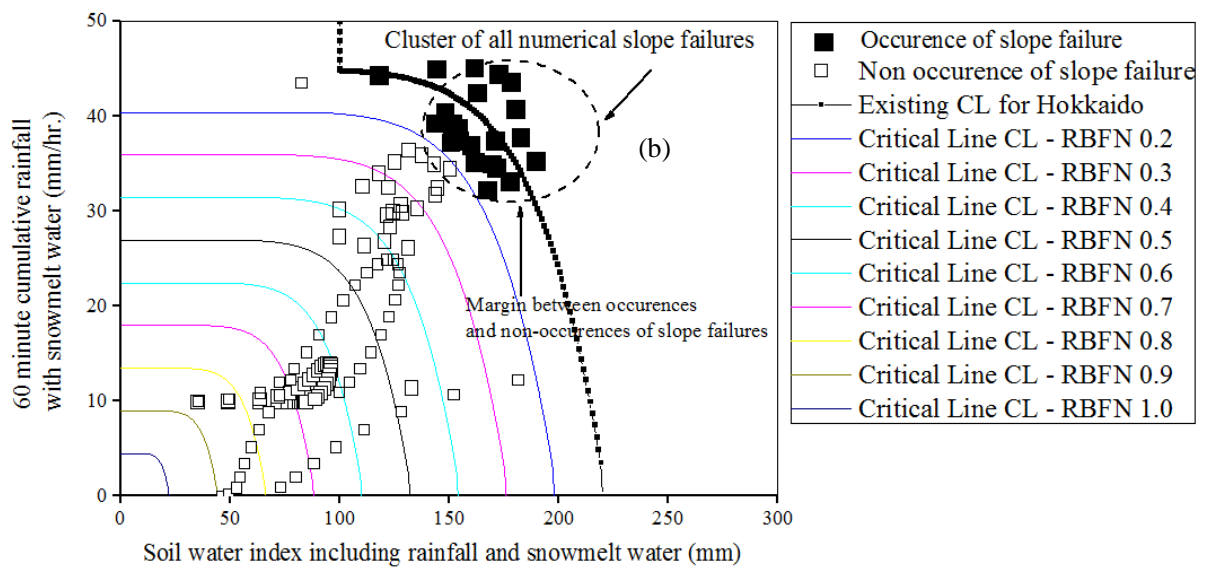
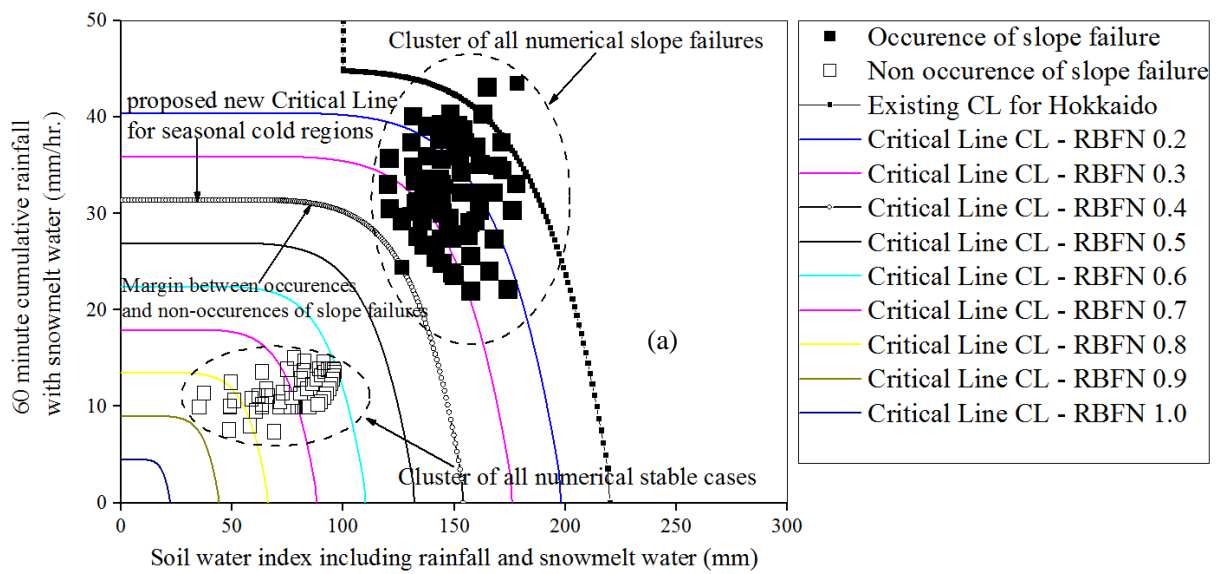


Figure 23 Possible revisions of the Critical Line designated for Hokkaido

Revision threshold lines are conceptual/equivalent RBFN lines (a) series B and C, (b) series A and D.

Table 1 List of sediment disasters occurred and recorded in snowy cold regions of Japan (after Iwakura et al. 2010)

S. No.	Date of occurrence (dd-mm-year)	City	Type of sediment-related disasters	Cause
1	01-04-1999	Lee County	Landslides	Snow melting
2	14-04-1999	Otaru City	Landslides	Rainfall and snow melting
3	15-04-1999	Shakotan-gun	Landslides	Snow melting
4	18-04-1999	Kamikawa-gun	Landslides	Snow melting
5	01-05-2000	Nakayama pass	Landslides	Rainfall and snow melting
5	22-02-2004	Western County	Landslides	Rainfall and snow melting
6	22-02-2004	Western County	Sediment discharge	Rainfall and snow melting
7	17-03-2004	Western County	Debris flow	Rainfall and snow melting
8	17-03-2004	Kodaira County	Landslides	Rainfall and snow melting
9	30-04-2007	Otaru	Debris flow	Snow melting
10	02-05-2007	Otaru	Landslides	Snow melting
11	01-05-2012	Nakayama pass	Sediment discharge	Rainfall and snow melting
12	07-04-2013	Nakayama pass	Embankment collapse	Rainfall and snow melting

Table 2 Different initial conditions chosen for analysis based on different seasons from the numerical simulation (Siva Subramanian et al. 2017)

Study series	Day	Date	Characteristics
A	100	16-02-2013	During freezing
B	150	07-04-2013	During thawing
C	200	27-05-2013	After thawing
D	343	16-10-2013	Before freezing

Table 3 Analytical conditions, summary of combination of factors and independent variables used in parametric studies

Study series	Slope angle α (°)	Slope heights H (m)	Rainfall rates P_r (mm/hr.) and duration (hours)	Snowmelt rates P_s (mm/hr.)
A	30	5	(a) 10 (00:00 to 23:00)	
B	35	10	(b) 30 (00:00 to 06:00)	(i) 0
C	40	15	(c) 30 (06:00 to 12:00)	(ii) 0 to 4
D	45	20	(d) 30 (12:00 to 18:00)	(iii) 0 to 15
			(e) 30 (18:00 to 24:00)	

Note: 4 Initial water content distributions, 4 slope angles, 4 slope heights, 5 rainfall rates and 3 snowmelt water rates = $4 \times 4 \times 4 \times 5 \times 3 = 960$ numerical simulations

Table 4. Different combinations of rainfall (P_r) and snowmelt rates (P_s) considered.

S. No	Rainfall amount (mm/hr.)	Duration	Type
1	10	24 hours	Continuous
2	30	6 hours	Continuous
S. No	Snowmelt rate (mm/hr.)	Duration	Type
1	0 ~ 4	24 hours	Sinusoidal (Max. at 12:00)
2	0 ~ 15	24 hours	Sinusoidal (Max. at 12:00)

Table 5. Rates of successful predictions (proper identification of the slope failure) using EP index (CL – Matsuura) with different half-lives.

S. No.	Study series	Slope failures	Stable cases	% of prediction EP (1.5 hr. and 72 hr.)		% of prediction EP (1.5 hr. and 24 hr.)		% of prediction EP (1.5 hr. and 6 hr.)	
				Success	Unsuccessful	Success	Unsuccessful	Success	Unsuccessful
1	A	0	240	-	-	-	-	-	-
2	B	224	16	100 %	0 %	86.66 %	13.33 %	86.66 %	13.33 %
3	C	224	16	100 %	0 %	86.66 %	13.33 %	86.66 %	13.33 %
4	D	64	176	100 %	0 %	100 %	0 %	100 %	0 %

Table 6. Rates of false predictions (stable cases identified as slope failures) using EP index reference to CL – Matsuura and CL3 - Yano.

S. No.	Study series	Slope failures	Stable cases	% of false predictions EP (1.5 hr. and 72 hr.) CL – Matsuura	% of false predictions EP (1.5 hr. and 72 hr.) CL3 - Yano
1	A	0	240	100 %	0 %
2	B	224	16	0 %	0 %
3	C	224	16	0 %	0 %
4	D	64	176	100 %	0 %

Table 7. Rates of successful predictions (proper identification of the slope failure) using SWI before and after revising CL.

S. No.	Study series	Slope failures	Stable cases	% of prediction by SWI before revising CL		% of prediction by SWI after revising CL	
				Success	Unsuccessful	Success	Unsuccessful
1	A	0	240	-	-	-	-
2	B	224	16	0 %	100 %	92.85 %	7.15 %
3	C	224	16	0 %	100 %	92.85 %	7.15 %
4	D	64	176	100 %	0 %	100 %	0 %

Table 8. Rates of false predictions (stable cases identified as slope failures) using SWI before and after revising CL.

S. No.	Study series	Slope failures	Stable cases	% of false prediction by SWI	
				before revising CL	after revising CL
1	A	0	240	0 %	100 %
2	B	224	16	0 %	0 %
3	C	224	16	0 %	0 %
4	D	64	176	0 %	100 %